Journal of Structural Geology, Vol. 9, No. 2, pp. 159 to 180, 1987
Printed in Great Britain

0191-8141/87 $03.00 + 0.00

Ductile and brittle deformations in the northern Snake Range, Nevada

YVES GAUDEMER and PAUL TAPPONNIER

Laboratoire de Tectonique, Mécanique de la Lithosphère, Institut de Physique du Globe de Paris, 4, place Jussieu, 75230 Paris Cedex 05, France

(*Received* 7 *October* 1985; *accepted in revised form* 30 *June* 1986)

Abstract—The northern Snake Range, east-central Nevada, is one of the metamorphic core complexes of the Sevier hinterland. Within the range a major décollement separates an 'upper plate' composed of brittlely deformed Paleozoic sedimentary rocks (mostly carbonates), from a 'lower plate' composed of metamorphic Upper Precambrian–Lower Cambrian rocks, intruded by gneissic granites. A study of the geometry and kinematics of structures and fabrics at outcrop scale and in thin sections indicates that: the northern Snake Range décollement has been a zone of intense non-coaxial E-vergent shear and transport in a ≃ N115°E direction. Outstanding asymmetric boudinage within the marble sheet capping the lower plate testifies for late ductile shear strains (γ) of at least 20. The interface between brittlely and ductilely deformed rocks seems too sharp to represent a regional rheological transition, but might result from two distinct phases of deformation. Ductile deformation in and below the décollement could have occurred before brittle deformation in the upper plate. Brittle faulting in the upper plate related to Basin and Range extension reactivated the upper surface of the ductile shear zone. High topographic relief on the normal faults bounding the range triggered the slide of olistolites from the upper plate into the adjacent Oligo-Miocene basins.

INTRODUCTION

THE NORTHERN Snake Range is a metamorphic core complex of the Basin and Range province, an area of complex tectonic history (e.g. Coney 1980) (Fig. 1). Its present geometry, as an uplifted block of mostly Upper Precambrian to Middle Paleozoic sedimentary and igneous rocks surrounded by late Tertiary to Quaternary sediment-filled basins, is the result of the latest stage in that history: the post-Upper Oligocene–Lower Miocene extensional tectonics which has affected much of the western United States, particularly Nevada (e.g. Stewart 1978). In recent years, geologists have paid special attention to the northern Snake Range because of a peculiar structure revealed by this late Tertiary uplift: the northern Snake Range décollement (NSRD). The NSRD is a flattish, sharp discontinuity dividing the range into:

(i) a 'lower plate' consisting of metamorphosed Upper Precambrian and Lower Cambrian clastic sediments, mostly quartzites and schists, locally intruded by commonly gneissic granite bodies; and

(ii) an 'upper plate' consisting of more brittlely deformed (by normal faults) Paleozoic limestones and dolomites, with some interbedded shale layers.

A marble sheet, the marble tectonite of Misch (1960), marks the décollement in the eastern part of the range (Figs. 1 and 2a). The NSRD has been variously interpreted as a major thrust related to Nevadan (Mesozoic) crustal shortening (e.g. Misch & Hazzard 1962), as a Tertiary denudation fault (Armstrong 1972, Coney 1974), as a Tertiary transcrustal low-angle normal fault (Wernicke 1981), and as a regional brittle–ductile transition during Tertiary extension (Miller *et al.* 1983). So far, however, comparatively little detailed work has been done on the nature and styles of the strains suffered by the different rocks in the Range. We present here new observations of small structures in the lower and upper plates and in the layers of tectonites associated with the NSRD, which allow the geometry and kinematics of deformations at the outcrop scale to be determined. Field measurements were complemented by laboratory analysis of preferred lattice orientations in quartz-rich rocks of the lower plate. We discuss the relationships between small scale deformation patterns and structures observed and mapped at the scale of the entire range (e.g. Wernicke 1981, Miller *et al.* 1983), as well as the compatibility between such deformation patterns and the alternative interpretations proposed so far.

DUCTILE DEFORMATION IN LOWER PLATE ROCKS

Throughout the range, in the metamorphic rocks of the lower plate, ductile deformation is characterized by a metamorphic foliation in general parallel to the original bedding (e.g. Miller *et al.* 1983, fig. 5). The foliation follows the flattened dome-shape of the range: subhorizontal in its inner part, it dips gently up to 25–30° outwards on the western and eastern sides (Fig. 2a). This general attitude is outlined by the marble layer which caps the lower plate (Fig. 2a). Locally, however, the foliation and the marble layer dip more steeply as, for instance, in Smith Creek Canyon (Fig. 1) where they dip 40°NNE. Also, between the upper reaches of Negro Creek, and those of Hendrys and Smith Creeks (Fig. 2a), the marble layer dips up to 10–20°W, which accounts for the lower elevation at which the NSRD crops out in Negro Creek (Figs. 1 and 2a) (see also fig. 2 in Miller *et al.* 1983). The foliation planes contain a generally strong

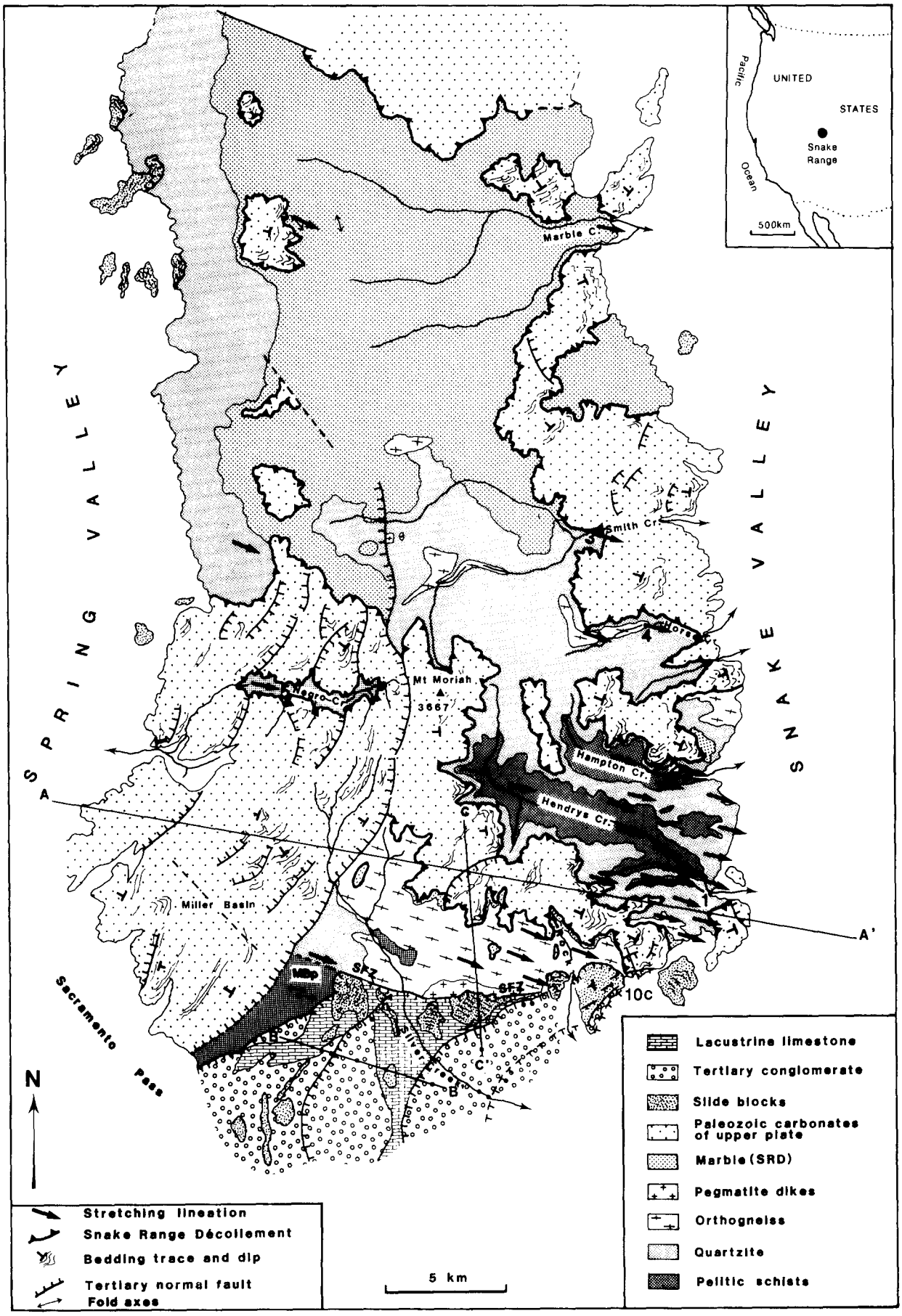

Fig. 1. Schematic structural map of northern Snake Range, largely based on work by Gans & Miller (1983), Grier (1983), Miller *et al.* (1983), and Stewart & Carlson (1978) and including our microstructural observations as well as inferences from NHAP photos (high altitude photographs, scale ≃1/60,000). Only major units and structures are shown, particularly in upper plate. Numbers indicate sites where samples were collected for preferred lattice orientation measurements. AA', BB' and CC' refer to cross-sections of Figs. 2(a) and 10.

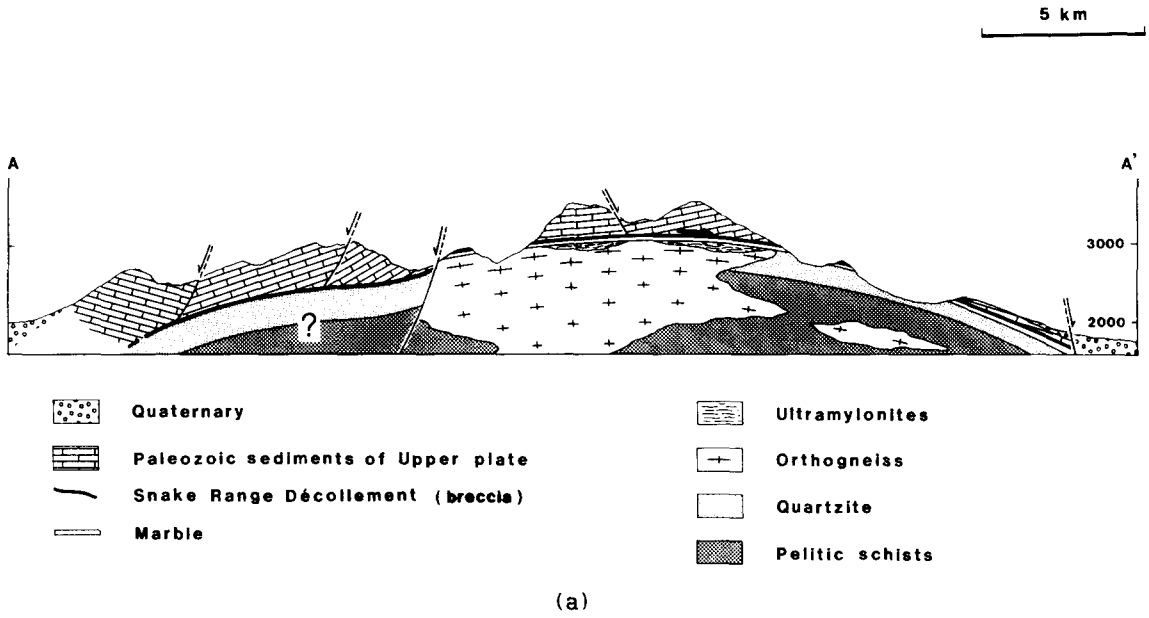

(a)

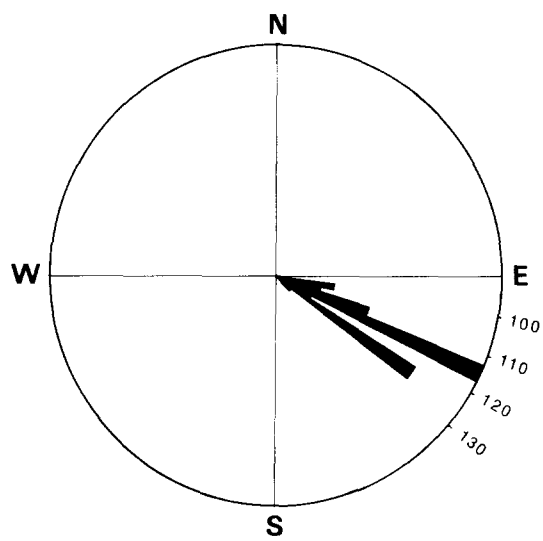

(b)

Fig. 2. (a) Schematic cross-section along profile AA' (Fig. 1). (b) Rose diagram of trends of stretching lineations in lower plate and marble sheet of northern Snake Range (97 measurements, each an average from a flattish foliation surface a few square metres in area, Fig. 1). Maxima at N115°E and N125°E probably result from bias of larger number of measurements in areas of range where most work was done.

stretching lineation of rather constant trend throughout the range: N115°E ± 15° (Fig. 2b) (e.g. Miller *et al.* 1983, fig. 5). At a more detailed level, the trend of the lineation swings uniformly from N105°E in the north to N125°E in the south of the Range (Fig. 1). The geometry, kinematics and amounts of ductile strain in the lower plate are particularly clear within quartz-rich Upper Precambrian to Lower Cambrian rocks and gneissic granites.

Deformation in McCoy Creek pelites and Prospect Mountain quartzites

In Hendrys Creek Canyon (Fig. 1), the layer of garnet-amphibole schists which belongs to the pelitic Precambrian McCoy Creek group exhibits a well developed foliation S_1, parallel to the bedding S_0. A strong stretching lineation is marked by dark amphiboles, elongated in a N110°E direction. An incipient schistosity S_2 cuts S_1, and dips 20°W while S_1 dips approximately 10°E. Polyhedral garnets, about 1–2 mm in diameter, deflect S_0 and S_1. The asymmetry of that deflection, the inclination of S_2 with respect to S_1 and the well-developed lineation in S_0-S_1 are consistent with a non-coaxial progressive strain regime, involving a large component of E-vergent shear. Measurements of aspect ratios (8:1:0.1) of stretched pebbles in rocks of the McCoy Creek group in this area (Miller *et al.* 1983) indicate shear strains γ on the order of 10.

A similar strain regime is clear in the Prospect Mountain quartzites. In Hendrys Creek and Hampton Creek (Fig. 1) the well-developed foliation has caused splitting of the quartzites into slabs, the thickness of which increases from top to bottom of the quartzite pile. This increase may be indicative of a decrease in deformation intensity with depth. The horizontal surfaces of the quartzite slabs are covered with muscovites and phengites, the long axes of which parallel the strong N115°E stretching lineation. In Hendrys Creek, the foliation is affected by open meter to decameter-scale folds, the axes of which trend parallel to the lineation, as noted by Rowles (1982) in Hampton Creek, and by Coney (1974).

The non-coaxial style of deformation in the quartzites is shown by the analysis of preferred lattice orientations in oriented samples from the eastern part of the range (Fig. 3a). Measurements at four sites (Fig. 4a) yielded distributions of quartz ⟨*c*⟩ axes in girdles tilted towards the east with respect to the plane perpendicular to the lineation, compatible with a mechanism close to E-vergent simple shear (Bouchez 1977, Gapais 1979, Laurent & Etchécopar 1976). The presence of a maximum close to the *Y* axis, commonly interpreted as resulting from gliding along prismatic planes in the ⟨*a*⟩ direction (e.g. Bouchez 1977), is indicative of relatively high temperature conditions. At the fifth site however, in Negro Creek (Fig. 1), a different distribution of ⟨*c*⟩ axes is observed with two ill-defined crossed girdles (Fig. 4b), suggesting a predominant component of coaxial deformation. Texture goniometer analysis of the distribution of ⟨*a*⟩ axes confirms the flattening component, but suggests also a small component of E-directed shear, as indicated by the eastward dip of the average plane *Z'* (Fig. 4c) (Gapais 1979). In the field and in thin section, the quartzites of Negro Creek appear to be less deformed than those which crop out on the eastern side of the range: the stretching lineation in particular is less well-developed than at most other sites (e.g. Hendrys Creek Canyon).

Deformation in the gneisses

Several granitic intrusions are found in the northern Snake Range (Fig. 1), and many, if not all, are gneissic. The largest gneiss body crops out on the southern side of the range, where it has widely intruded the Prospect Mountain quartzites.

The foliation planes (*S*) in the gneisses are well marked by mica layers and flattened feldspars. The foliation maintains a constant attitude as it passes from the gneiss to the intruded quartzite. This is particularly clear in Horse Canyon (Fig. 1), where the contact is a zone of intimately imbricated sheets of gneiss and quartzite, each a few metres thick. Everywhere, asymmetric pressure shadows where quartz has recrystallized indicate that large K-feldspars have rotated (Fig. 3b). The rotational component of deformation is consistent with E-vergent shear (Malavieille *et al.* 1981, Simpson & Schmid 1983). The gneisses also exhibit a set of planes which dip 15–20° more eastwardly than the foliation (Fig. 3b). These discrete plates, which are regularly spaced (≈1 cm) and marked by quartz ribbons and thin (≈1–2 mm) layers of biotite, have also accommodated E-directed shear and correspond to *C'* planes in the sense of Berthé *et al.* (1979) (Fig. 3b) (see also Simpson & Schmid 1983, Lister & Snoke 1984). This widespread pattern of deformation indicates that the granite bodies were gneissified in a strong E-vergent shear regime. Dioritic inclusions in the granite bodies are less deformed than the granites. Lamellae of feldspars, biotite and amphiboles within them, however, are parallel to the foliation in the surrounding gneiss. As observed by other authors (Nelson 1969, Miller *et al.* 1983) the greater development of the foliation and lineation near the NSRD implies a decrease in the amount of finite strain in the gneisses and the quartzites with increasing depth below the NSRD.

DUCTILE DEFORMATION WITHIN THE DECOLLEMENT

The layer of tectonite, up to more than 100 m thick, which outlines the NSRD (Fig. 2a) (Misch & Hazzard 1962, Nelson 1969, Wernicke 1981) corresponds to an outstanding shear zone, in which high strains are localized. The nature and intensity of such strains are particularly clear within two units of the tectonite layer.

Sheath folds and ultramylonites in Rock Canyon

In the vicinity of Rock Canyon (Fig. 1), a strongly folded layer of thinly bedded calc-silicate rocks separates the gneisses from the NSRD marbles. Fold axial planes are generally horizontal, and most fold axes strike N125°E, parallel to the stretching lineation (Fig. 5b). Sheath folds are well developed everywhere in this layer (Fig. 5a). This indicates shear strains of large magnitude ($\gamma \geq 10$) (e.g. Cobbold & Quinquis 1980, Lacassin & Mattauer 1985). The presence of large boudins of aplite with asymmetric tails several m long is also consistent with large amounts of eastward transport. This sense of movement is corroborated by pervasive boudinage at a smaller scale. Finally, folds parallel to the stretching lineation, and spectacular sheath folds are observed in a thinly laminated ultramylonite zone, a few metres thick, at the base of the marbles.

Snake Range marble sheet

The highly heterogeneous deformational style described above, which contrasts with the relatively homogeneous strains observed in the pelites, quartzites and gneisses within the lower plate, is also typical of deformation in the marble layer at all scales: ductile faults, folds and boudins from tens of cm to hundreds of m in size, can be observed everywhere. In many places, the deformation is dominated by isoclinal folds, the axes of which trend from N70°E to N130°E, but are commonly parallel to the stretching lineation (≈N115°E). Such is

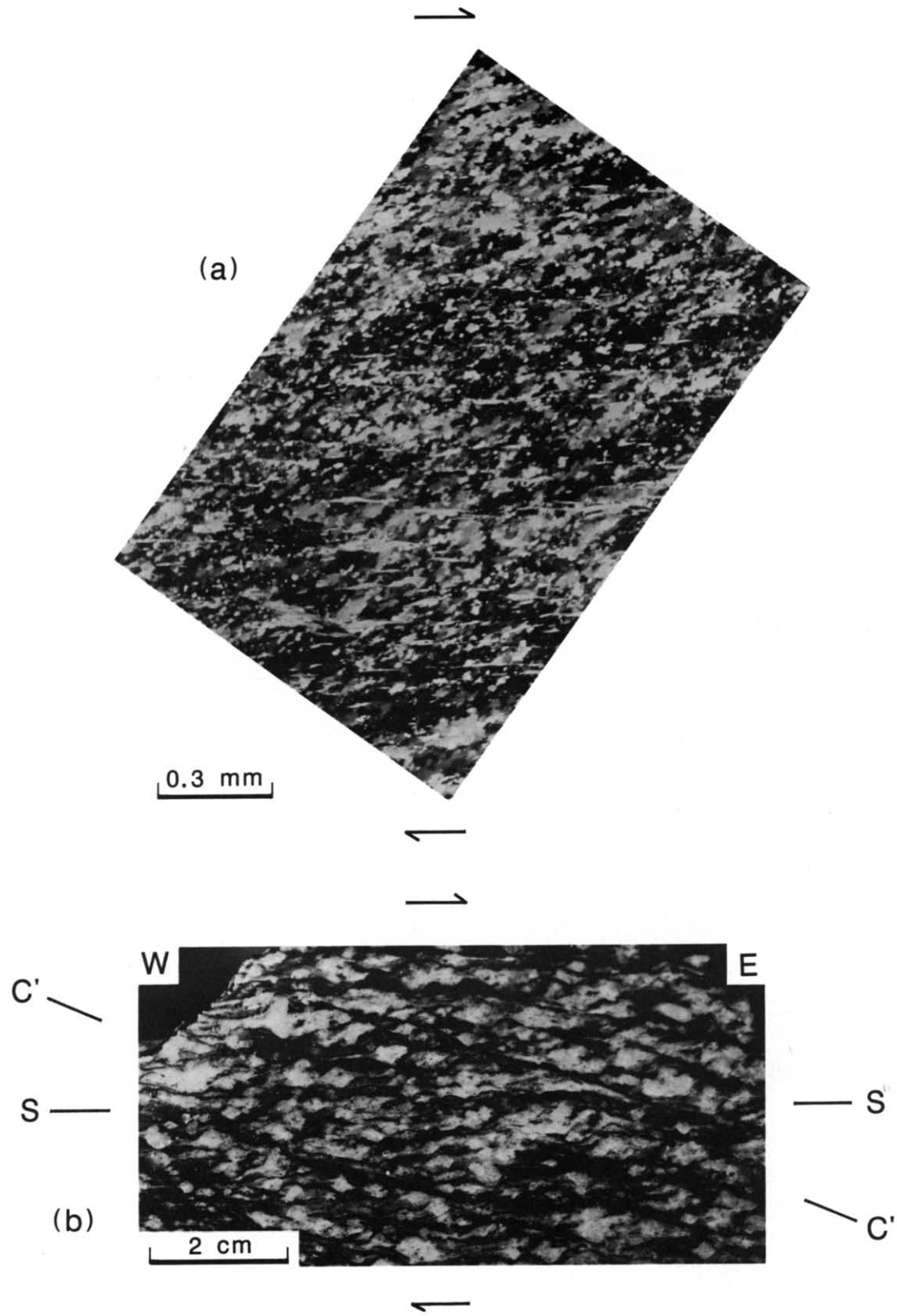

Fig. 3. (a) Photomicrograph of quartzite sample from Smith Creek (site 3 on Fig. 1). (b) S and C′ planes in gneisses from Horse Canyon (Fig. 1).

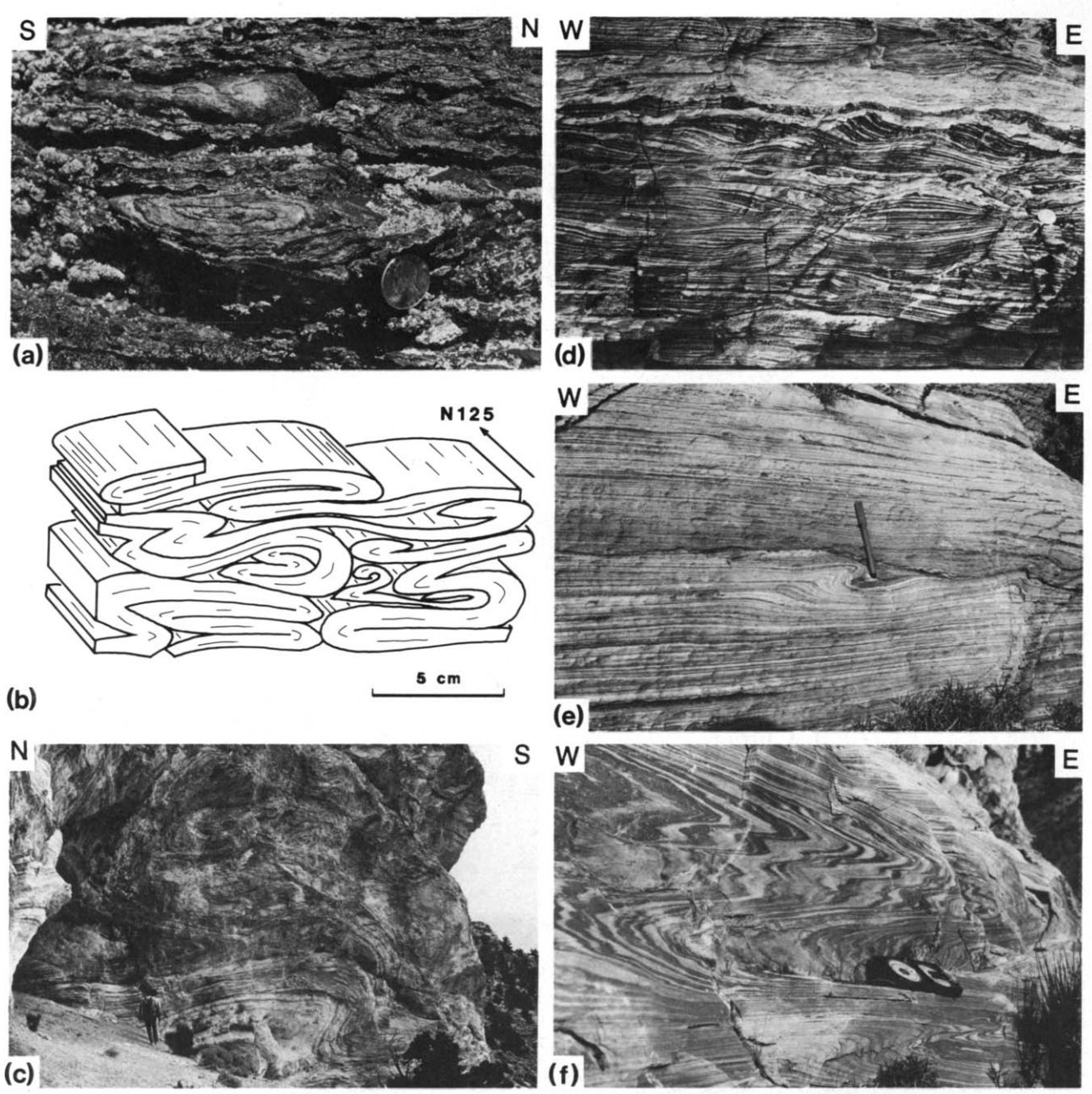

Fig. 5(a). Sheath folds in calc-silicate layers beneath NSRD marble sheet in Rock Canyon. Scale is given by coin in lower right corner. (b) Folds with axes parallel to lineation in calc-silicates. Same location as (a). (c) Large folds with axes parallel to stretching lineation in NSRD marble sheet above Rock Canyon. (d) W-dipping shear zones (strain-slip cleavage) in lower limb of fold in marble layer M2 (Fig. 7, lower right). (e) Incipient folding in marble layer M4. (f) Folding in marble layer M4.

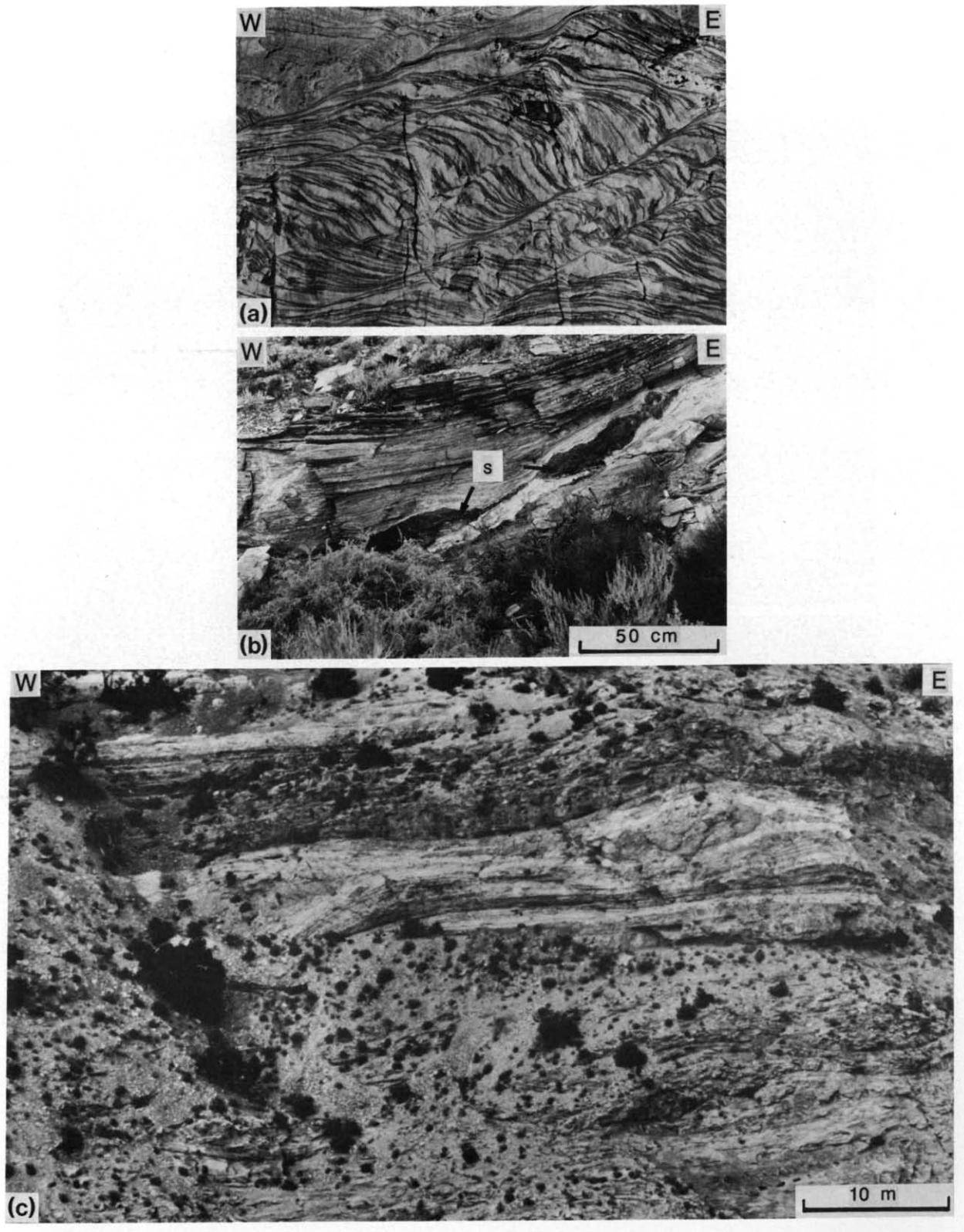

Fig. 8. (a) Secondary W-dipping shear zones in marble layer M4 (Marble Canyon). (b) Secondary W-dipping shear zone offsetting kersantite sill (s) in wake of large dolomitic boudin. Photograph flipped so that east is on right side of page (Marble Canyon). (c) Asymmetry of decameter-scale dolomitic boudins (Marble Canyon).

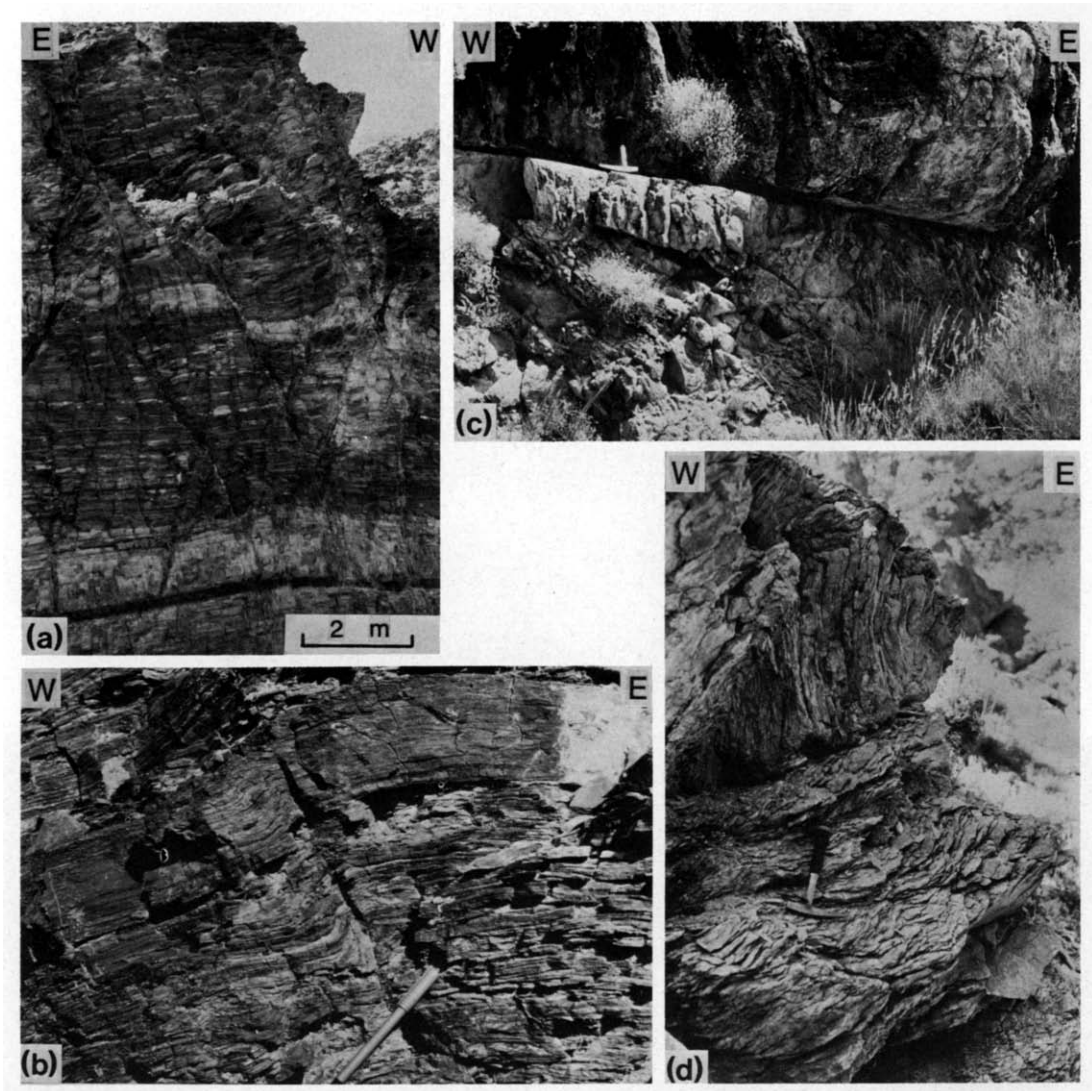

Fig. 11. (a) Conjugate high-angle brittle normal faults and en-échelon vertical joints in the lower plate (McCoy Creek group pelites, Hendrys Creek). (b) Reverse fault drag in top layer of mylonitic marble (Marble Canyon). (c) Close-up of planar low-angle normal fault of Fig. 12(a). (d) Folded stylolitic cleavage and west-dipping reverse faults in recrystallized limestones above NSRD foliated marbles (Smith Creek).

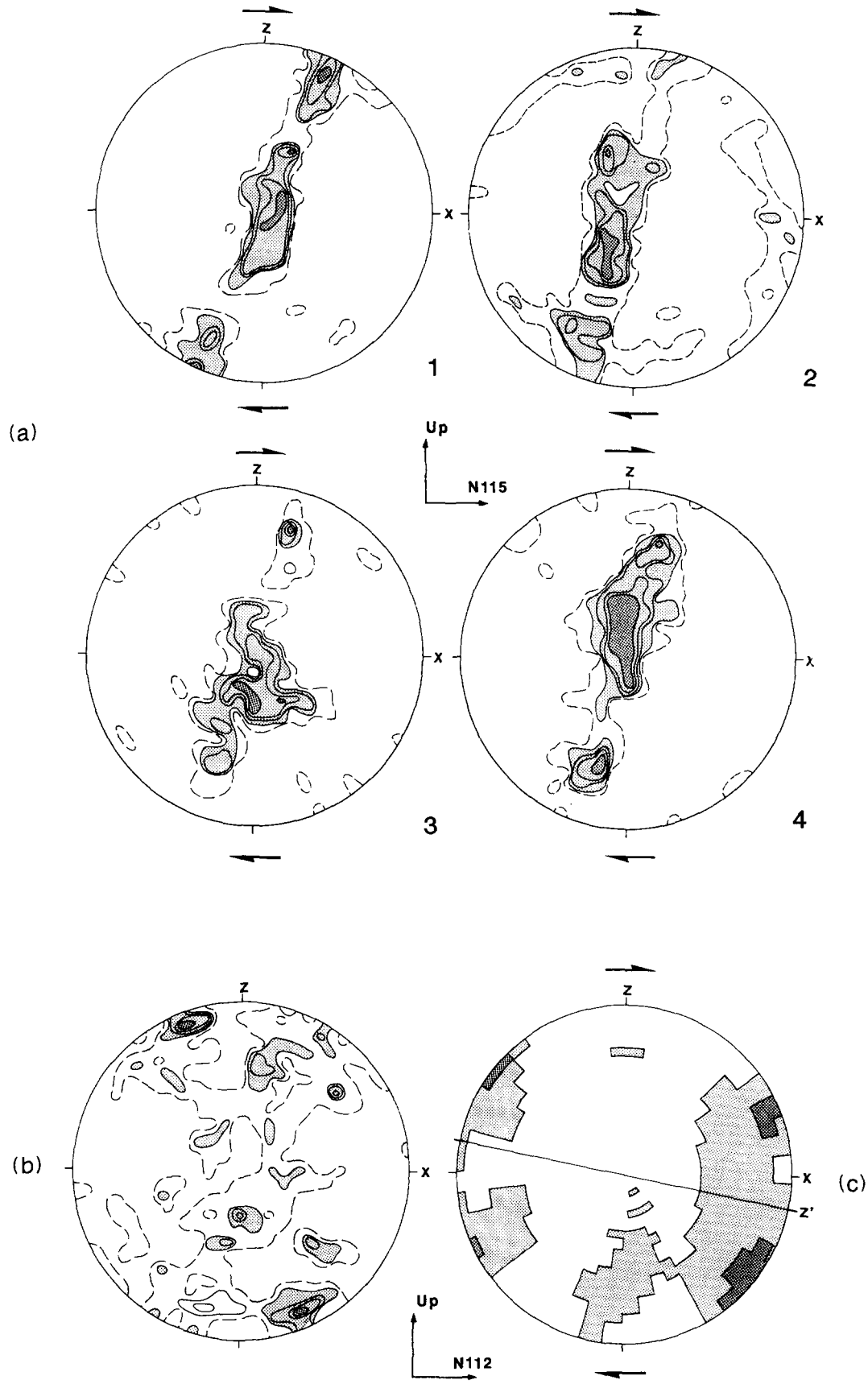

Fig. 4. (a) Typical pattern of preferred orientation of quartz ⟨*c*⟩ axes in quartzites from (1) Hendrys Creek, (2) Hampton Creek, (3) Smith Creek, and (4) Horse Canyon (see locations on Fig. 1). Contours are 0.5%, 0.9%, 1.4%, 1.8% and 2.7% of points per 1% of area. *X* is direction of stretching lineation in foliation plane, *Z* is perpendicular to foliation plane. (b) Typical pattern of preferred orientation of ⟨*c*⟩ axes in quartzites from Negro Creek (5); symbols as in (a). (c) Preferred orientation of ⟨*a*⟩ axes in Negro Creek [same sample as (b)] obtained by texture goniometry. Light stipple: ≥0.46%, dark stipple: ≥1.14% of mean diffracted intensity.

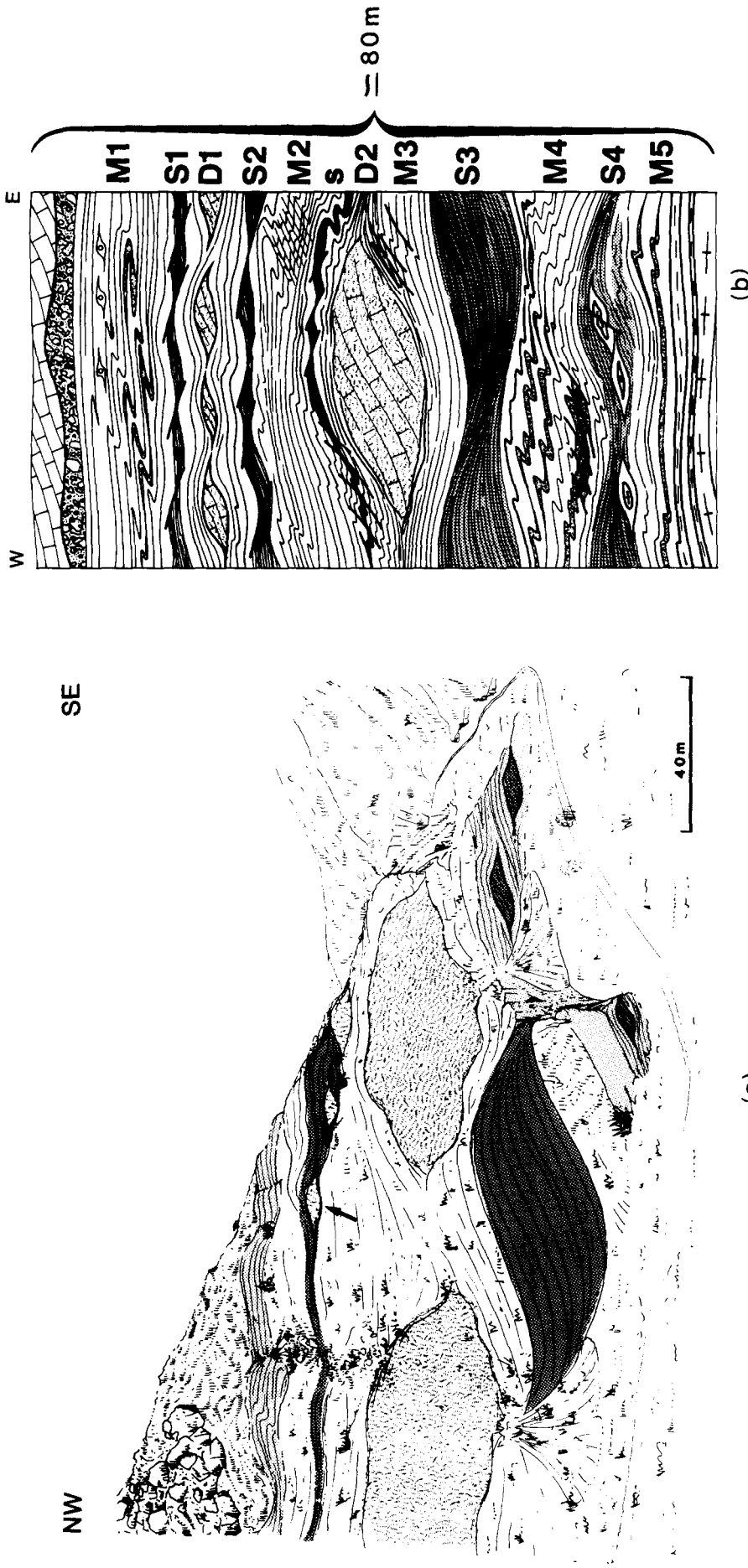

Fig. 6. (a) Typical view of tectonic layering and asymmetric boudinage in Marble Canyon. Small dolomitic boudins (arrow) are about 10 m long. (b) Schematic vertical section of tectonic layering and boudinage in Marble Canyon (layers described in text).

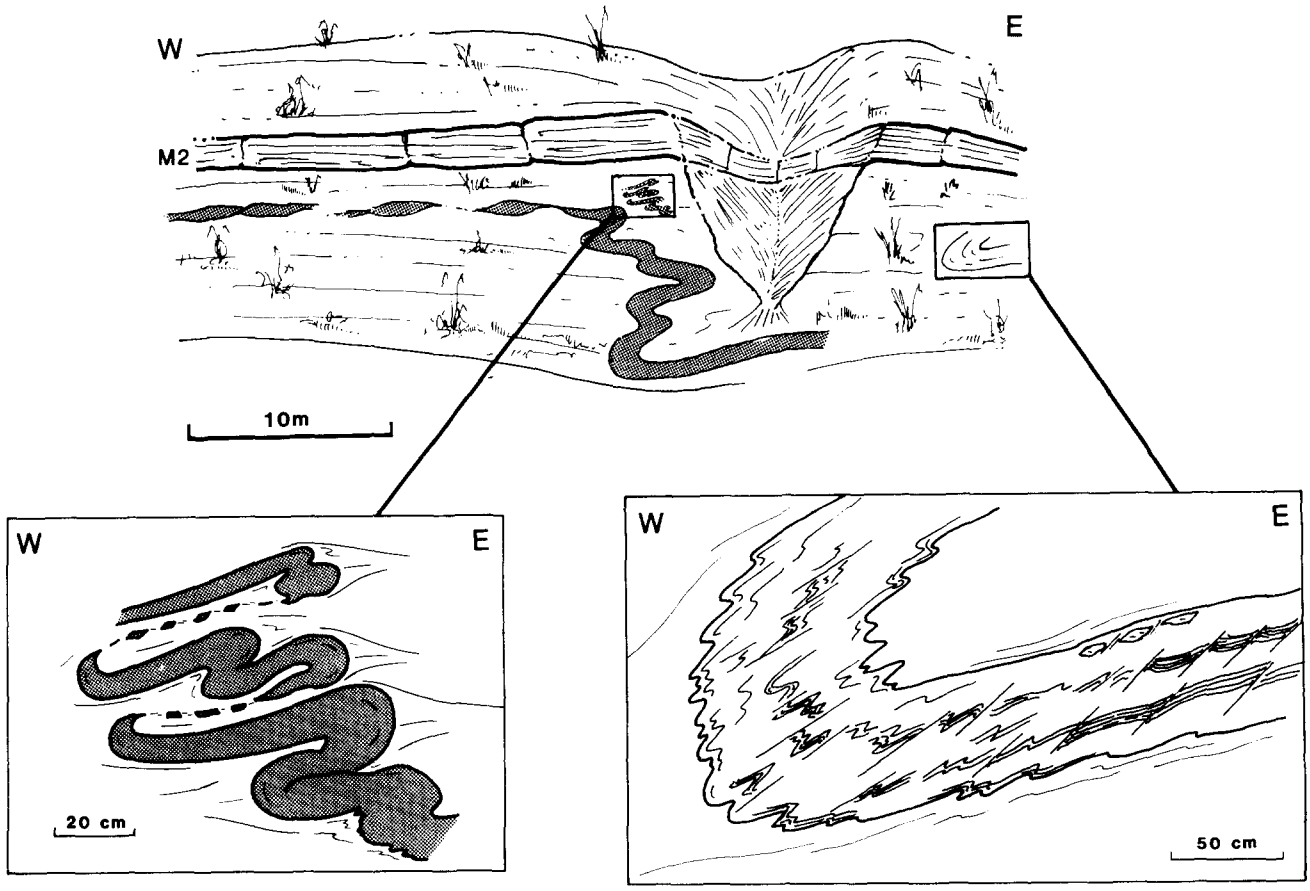

Fig. 7. Folds with axes at high angles to the stretching lineation. Lower left insert: folding of small kersantite sill; lower right insert: fold hinge in marble layer M2.

the case for the large folds in Fig. 5c, above Rock Canyon for instance. Strain patterns in the marble are best exposed in the northeastern part of the range, in a shallow canyon (Marble Canyon) whose gentle slope follows the décollement level. Marbles in Marble Canyon show a conspicuous structural 'layering', both on a large and a small scale (Fig. 6). This layering, previously recognized by Nelson (1969) is found in much of the marble sheet in the northernmost part of the Snake Range, and in a similar marble sheet in Kern Mountains and Deep Creek Range to the North. Individual layers may be followed for at least 5 km upstream in Marble Canyon. Most of them display rotational boudinage (Fig. 6). This uniform layering is summarized in Fig. 6(b). From a structural point of view, one may distinguish, from top to bottom (Fig. 6b). (1) A first layer of siliceous blue–gray marbles (M1) with a well-defined stretching lineation striking N105°E. The foliation is affected by isoclinal folds, the axes of which trend parallel to this lineation. Small, more quartzitic inclusions and boudins within the marble layer have asymmetric pressure shadows. The marbles contain at least one layer of dark brown schists (S1) (Nelson 1969), at most a few metres thick, often boudinaged by E-dipping shear planes (Fig. 6b). (2) A first layer of massive dolomitic limestone boudins (D1), tens of metres in size (Fig. 8c), embedded in white–pink marbles which delineate large asymmetric tails. (3) A second layer of blue–gray marbles (M2) containing a sheet of dark brown schists (S2) and a boudinaged or folded sill of mafic rocks (s) (amphibolites) (Figs. 6 and 7), identified by Nelson (1969) as a metamorphosed kersantite sill. (4) A second layer of large dolomite boudins (D2), at places up to several tens of metres in length, bulky enough to cause changes in the dip of all the upper layers of marbles in the canyon (Fig. 6). (5) A third layer of laminated blue–gray marbles (M3). (6) A layer of greenish brown calc-schists (S3) which can be 10–20 m thick. The foliation in the calc-schists is boudinaged by E-dipping shear zones. (7) A fourth layer of laminated white and bluish gray marbles (M4) which exhibit particularly outstanding folds and shear zones. (8) A layer of greenish brown calc-schists (S4) analogous to S3, albeit thinner, containing boudins of granitic rocks (mostly pegmatites) near its base. (9) Laminated bluish gray marbles (M5) on top of white vitreous quartzites and schists showing a strong N112°E stretching lineation.

Asymmetric folding and boudinage; 'ductile normal' faults

All the observations we made in Marble Canyon at scales above 10 m, and the majority of such observations at a smaller scale, indicate E-vergent shear and imply large amounts of transport of the upper plate. While deformation of the white–blue banded marbles is the most homogeneous, individual layers being traceable without interruption for tens of metres, the foliation is

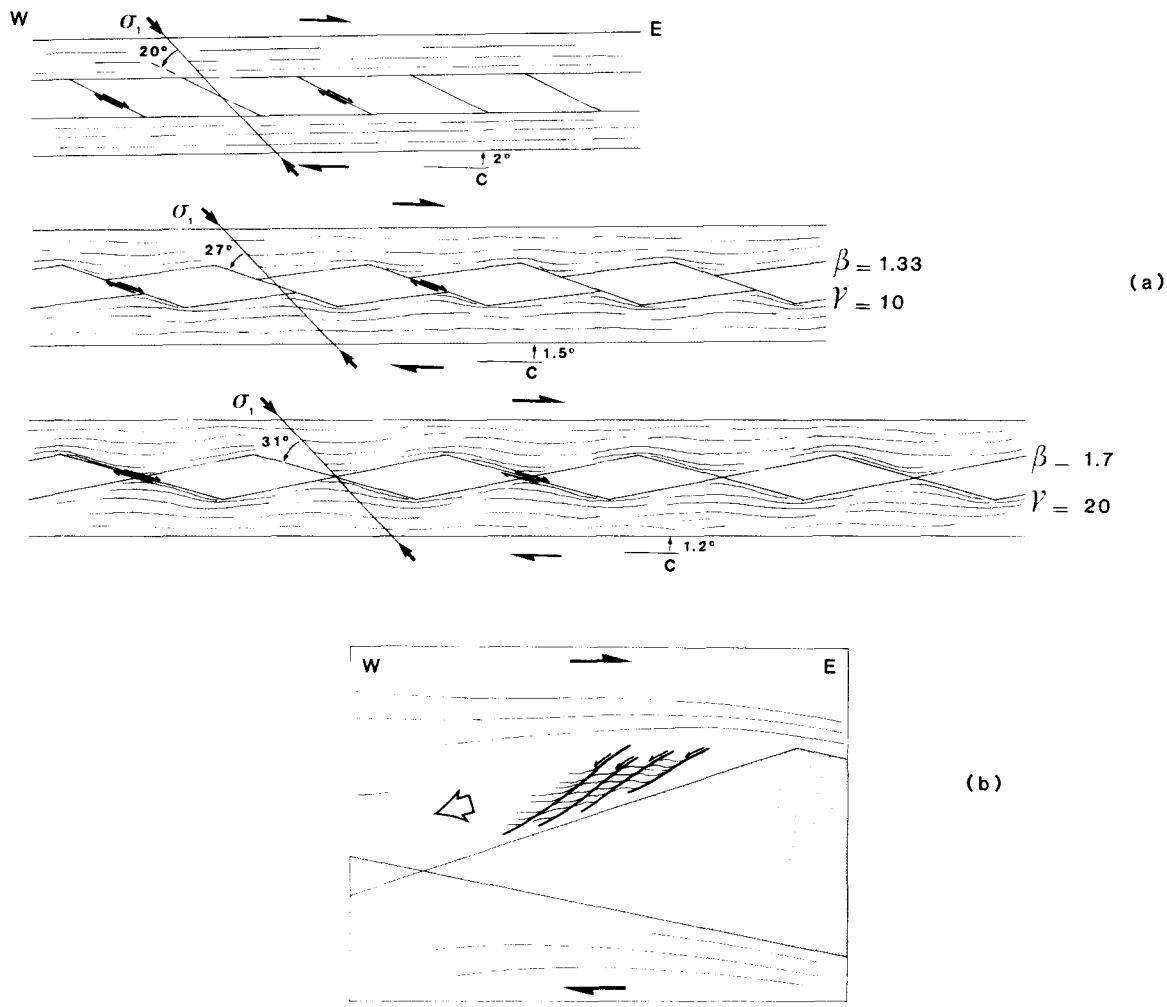

Fig. 9. (a) Development of boudinage by asymmetric extension of competent layer within more ductile ones in simple shear regime. Principal stress σ_1 is assumed to be at 45° to the simple shear plane C. Initial angle between C and foliation in ductile layers (shaded) and the more competent layer between them is assumed to be 2°. Brittle shear zones in the competent layer are assumed to form at a lower angle (20°) to σ_1. Brittle and ductile layers are stretched by the same amount during progressive shear (33% and 70% respectively for intermediate and final stages). Corresponding stretching factors, β, and shear strains are 1.33, 1.70 and 10 and 20 respectively. As foliation in the ductile layers rotates about 1° clockwise, brittle shears and boudins rotate about 10° anticlockwise. (b) Hypothetical development of W-dipping shear zones upstream of W-dipping edge of large rotating boudin.

affected in places by small folds, the formation of which was apparently triggered by small heterogeneities (Fig. 5e). Locally, some of the folds seem to evolve into small 'thrusts'. All of such folds, whose axes make angles of 30–40° with the regional stretching lineation, are overturned to the E (Figs. 5e & f). This is the case for the conspicuous folds observed in the kersantite sill (s) and one of its small offshoots in layer M2 (Figs. 6 and 7). In addition to the overall E-facing attitude of the folds, a W-dipping axial-plane cleavage is observed in the thickened hinges and the overturned limbs are strongly attenuated (Fig. 7 insert on the left). Above the folded sill, a similar asymmetric fold affects the white-gray, laminated marbles with brown-weathered interbeds of layer M2 (Fig. 7 insert on the right). Tight, second-order folds in that fold hinge have ≃ N–S striking, W-dipping axial planes, and the brownish layers in the lower limb are offset by discrete W-dipping planes which may be interpreted as strain–slip cleavage (Fig. 5d).

The ubiquitous, outstanding asymmetry of boudinage, both on a small and a large scale, also implies predominant non-coaxial, E-vergent shear strains (Fig. 6). This is clear either from the pressure shadows or tails around small quartzitic and dolomitic inclusions in layer M1 (Fig. 6b) (e.g. Malavieille 1982), from the larger tails of the massive dolomitic boudins, tens to hundreds of m in size, of layers D1 and D2 (Fig. 6b) or of the small pegmatitic ones in layer S4, from the E-dipping shear zones in the schists and calc-schists of layers S1, S2, S3 and S4 (Fig. 6), or from the shape of kersantite boudins where the sills have been truncated and sheared (Fig. 7). Most of the boudins, whether they are made of foliated marbles or schists, or of less ductile rocks such as dolomite, appear to have formed by down-to-the-east movement along shear zones dipping more steeply eastwards than the general foliation and layering.

One simple mechanism for generating such an asymmetric, rotational boudinage is depicted in Fig. 9(a): in a regime of steady-state, progressive simple shear, the maximum principal stress σ_1 may be expected to make

an angle of ≈45° with the orientation of the main ductile shear zone. Within a décollement such as NSRD, and for large enough strains ($\gamma > 10$), both the foliation and the original or shear-related layering will be nearly parallel to the shear plane. In such a shear zone, layers which are less ductile because of their composition (dolomite) or which become so because of strain hardening, may not deform in a purely plastic (isovolumetric) way. Instead, in such layers, shear is likely to occur within more brittle (dilatant) fault zones making an angle of less than 45° with σ_1. Only those faults which make a low angle with the main shear plane can maintain a rather stable attitude and sense with increasing strain and contribute to the lengthening of the less ductile layers, in compatibility with the overall simple shear regime. They may thus be expected to develop preferentially, truncating and offsetting those layers in the manner shown in Fig. 9(a). Such a mechanism, which is physically and kinematically analogous to one of several mechanisms suggested for the formation of C′ planes in mylonitic rocks (e.g. Platt 1984, Passchier 1984), would account for the predominance and ubiquity of E-dipping 'normal' shear zones at all scales, as well as the down-to-the-west, up-to-the-east tails of the boudins in the E-vergent NSRD shear zone (Figs. 6 and 9a). In Fig. 9(a), the normal shear zones form with an original dip of 25°E and rotate counterclockwise 11°, while the average layer plane rotates clockwise only 0.8°. Note that with the assumption that the adjacent layers experience the same amount of extension, the overall simple shear (γ) required to dissociate two neighboring boudins with aspect ratios of the order of 4 is larger than 20.

Despite the predominance of E-dipping, normal shear zones in the NSRD marble sheet however, ductile W-dipping normal faults are often found to offset the thin blue–white banding of layers M2 and M4 (Figs. 6b and 8a). Such faults generally vanish upwards and downwards into the foliation, thus isolating sigmoidal slabs of marble in which the banding tilts eastwards (Fig. 8a). In most cases, darker layers, although strongly attenuated, can be followed along these faults or shear zones (Fig. 8a). The kersantite sill (Fig. 8b) and small boudins of dolomitic marble in layer M1 are also offset down-to-the-west by such shear zones.

Most of the better exposed W-dipping normal shear zones we observed were located in the wake of large boudins (Figs. 6 and 8). This association suggests that such shear zones might be due to perturbations of the overall E-vergent shear by the large asymmetric boudinage illustrated in Fig. 9(a). The progressive, antithetic, rotation of large boudins could for instance produce growing resistance to E-directed flow in the blue–white, more ductile marble, and increase the flattening strain component in areas against the topmost or lowermost parts of the W-dipping sides of such boudins. The marble might thus be forced to flow out of these more intensely flattened areas towards the necked zones between adjacent boudins, along normal shear zones guided by the W-dipping sides of the boudins (Fig. 9b). In any event, our observations imply that the W-dipping normal shear zones (Fig. 9b) are secondary features in a strain regime in which the process illustrated in Fig. 9(a) is dominant.

BRITTLE DEFORMATION

Faulting along the edges of the range

Since the Snake Range, together with the Deep Creek Range, belongs to one of the many, roughly N–S trending, topographic highs of the Basin and Range Province, one expects it to be limited, as most such highs, by Tertiary to Quaternary normal faults on either side. Besides, the Snake and Deep Creek Ranges are the only ranges, within the Great Basin proper, to exceed 12,000 feet.

Evidence for Quaternary faulting along either edge of the Snake–Deep Creek Range is less conspicuous, however, than along most other ranges between the Sierra Nevada and the Wasatch Front (e.g. Ruby Mts, Toiyabee Range, Stillwater Range, Tobin Range . . .) (e.g. Wallace 1978a). Nevertheless, east of the southern extremity of Deep Creek Range, en-échelon Quaternary scarps (Hintze 1980) appear to outline the surface expression of a major buried normal fault (Wallace 1978b). Also, near Sacramento Pass, a prominent Neogene normal fault juxtaposes the Miller Basin Wash metamorphic pelites (MBp, Fig. 1) with Oligo-Miocene clastics (Miller *et al.* 1983). The existence of late Cenozoic, N-striking normal faults bounding the northern Snake Range on either side may be inferred from either COCORP profiles (Gans *et al.* 1985, Hauser 1985) or Bouguer gravity maps (Miller *et al.* 1983). Such faults, generally concealed by onlapping fan deposits, probably cut and offset the NSRD (Fig. 1), as depicted on recent sections (Miller *et al.* 1983, fig.9, Gans *et al.* 1985, figs. 2 and 3).

Along the northern edge of the Sacramento Pass reentrant, the NSRD also appears to be offset by a series of roughly E–W fault segments (hereafter referred to as the Silver Creek Fault Zone (SFZ), which separate the ductilely sheared lower plate rocks from Tertiary conglomerates and lacustrine limestones to the South (Fig. 1) (Grier 1983). The conglomerates and limestones are tilted up to about 50°W and offset 1–2 km by at least two large arcuate normal faults which merge with the SFZ (Grier 1983, Miller *et al.* 1983) (Figs. 1, section BB′, and 10a). Small conjugate normal faults in the conglomerates and bedding-parallel stylolites in the limestones are compatible with roughly E–W extension and vertical maximum principal stress before tilting.

Irregular blocks of various sizes are embedded within the lacustrine limestones (Figs. 1 and 10a) (Grier 1983). Some of the blocks are of km dimensions (Figs. 1, 10a & b), and all of them are composed of Paleozoic carbonates or, more rarely, of quartzites. Several blocks contain or are made of tectonic breccia with angular, highly shattered carbonate clasts (Grier 1983). Particularly large and abundant blocks are found along the northern edge of the Sacramento Pass basin where they partly mask the

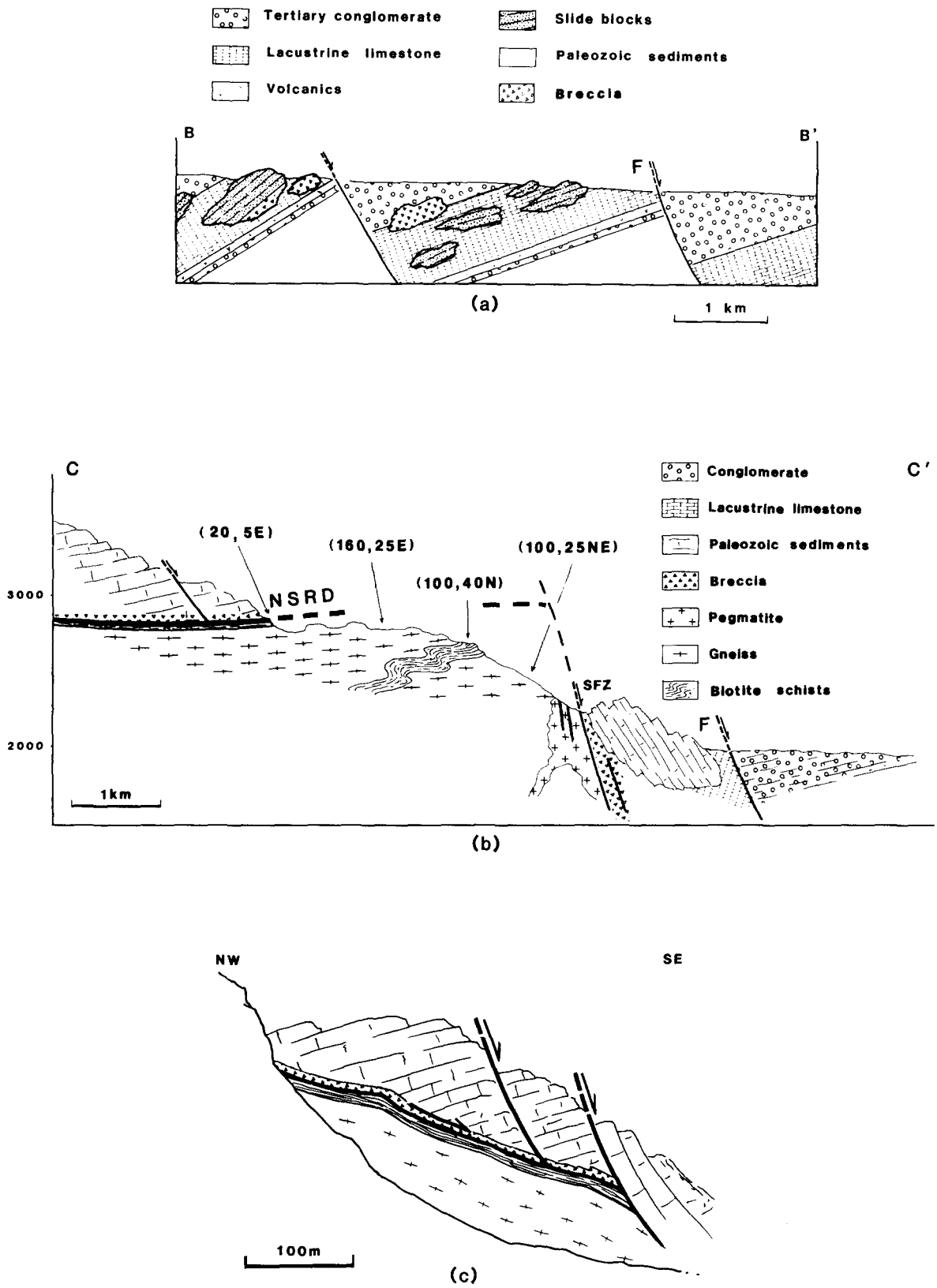

Fig. 10. (a) Schematic cross-section along profile BB′ in Sacramento Pass basin (location shown on Fig. 1) (based on mapping by Grier 1983). (b) Schematic cross-section along profile CC′ across southern boundary of northern Snake Range (location shown on Fig. 1). F points to a fault common to sections BB′ and CC′. Numbers are strikes and dips of foliation. (c) Red Ledge Canyon section (see b for legend) (location on Fig. 1).

SFZ. The bedding in most of these larger blocks dips steeply (up to 70°) to the SSW (Grier 1983) (Figs. 1 and 10b). As recognized by Grier (1983), all blocks appear to be slide blocks or olistolites. They seem to have slid from the uplifted edge of the upper plate down into an Upper Oligocene–Lower Miocene lake, mostly before the deposition of the thick upper conglomerates. This implies important topographic relief (Grier 1983) on probably steeply dipping faults at the time, particularly the SFZ. West of Silver Creek (Fig. 1), where the SFZ strikes ≈ N120°E, the linearity of its trace on National High Altitude Project (NHAP) photos is indicative of such steep dips, as well as of a component of strike–slip movement, probably left-lateral if coeval with normal faulting in the Sacramento Pass basin. East of Silver Creek, brittle deformation in the lower plate along the SFZ, here ≈E–W striking, is characterized by subvertical, N70–80°E trending, often chloritized fractures and faults and brecciated pegmatites (Fig. 10b). Tectonically brecciated quartzites and dolomites generally mark the base of the large slide blocks along the fault zone and separate them from rocks of the lower plate. Farther east, in Red Ledge Canyon (Figs. 1 and 10c), one segment of the same fault zone, outlined by a narrow band of limestones affected by a steep north-dipping, ≈N80°E striking fracture cleavage, appears to truncate the NSRD marbles and the lower plate, as depicted in Fig. 10(c).

The observations described here, which complement those presented in the maps of Grier (1983) and Miller *et al.* (1983), suggest to us that the SFZ cuts both the upper and lower plates of the northern Snake Range, displacing the NSRD shear zone and its characteristic marble sheet perhaps several km down to the south. This would fit the quantitatively constructed section CC′ (Figs. 1 and 10b) in which the NSRD marble sheet appears to vanish southwards and where foliation in the underlying gneisses keeps a constant, flattish attitude. The strong cataclasis linked with movement on the SFZ overprints that foliation and must have occurred after ductile shear in the lower plate and décollement. Since brittle displacement on the SFZ and on the normal faults which merge with it (Fig. 1) are probably coeval, ductile shear on the NSRD probably occurred prior to the extensional tectonics recorded in the Sacramento Pass basin. Thus, although the large westward tilts of the Tertiary sediments and the arcuate shape of the normal faults in the basin may be accounted for by soling of the latter faults on the NSRD at depth, the corresponding brittle displacements were probably only guided by the previously foliated, hardened top of the lower plate.

Brittle faulting within the Snake Range

In the metamorphic lower plate, significant brittle deformation overprints the ductile shear which has produced the foliation, lineation and boudinage. Although this brittle deformation is less spectacular than above the NSRD in the upper plate, it is pervasive. As noted by Miller *et al.* (1983, fig. 5f), the quartzites are cut in many places by vertical joints oriented N15°E, a direction roughly perpendicular to the direction of late Tertiary extension in most of the Basin and Range (WNW–ESE, Zoback *et al.* 1981). In addition to these vertical joints, the metamorphic pelites in Hendrys Creek show coeval, parallel and steeply dipping conjugate normal faults (Fig. 11a). Open cracks, oriented ≈N–S, are also found in the marbles. In a few instances however, brittle faults were observed to offset the ductile foliation in a way compatible with roughly horizontal shortening instead of extension. The ≈N–S striking, E-dipping reverse fault in the top layer of mylonitic marble in Marble Canyon (Fig. 11b) represents one example, and other such microfaults, striking N145°E, were found in the quartzites of Negro Creek.

Brittle deformation in the upper plate has been studied extensively, particularly in the southern part of the range (Miller *et al.* 1983). The Paleozoic carbonates are generally tilted, often towards the W (e.g. fig. 5c in Miller *et al.* 1983) (Figs. 1, 2a and 12b) and sliced by numerous low-to-high-angle normal faults whose average strike (N10°E ± 20°) is compatible with late Tertiary Basin and Range extension. The geometry of faulting however, as well as the bedding attitudes, appear to be less systematic than implied by the schematic or interpretative cross-sections of Miller *et al.* (1983), Bartley & Wernicke (1984), or Gans *et al.* (1985). In Smith Creek canyon for instance, the Paleozoic strata dip west only at the outlet of the canyon (Fig. 12a) and remain flat-lying or are tilted to the east upstream. Similarly, at the entrance of Negro Creek valley, bedding dips are mostly to the east. The two-phase kinematics (involving younger E-dipping normal faults offsetting older, now W-dipping faults tilted in a reverse attitude) documented in Duck Creek and Egan Ranges (Gans & Miller 1983) may characterize upper plate faulting in the southwestern part of the northern Snake Range (Miller *et al.* 1983, fig. 2). There are, however, prominent, presently normal, W-dipping faults as well in that area (Fig. 1). In fact, in areas where the upper plate extends to the edges of the range (e.g. Smith Creek outlet in Snake Valley and Negro Creek outlet in Spring Valley) normal faults near such edges generally dip towards the range front (e.g. Fig. 12a) while the faulted blocks are tilted towards the inside of the range (Figs. 1 and 12a).

High-angle normal faults within the upper plate often appear to sole into shallower-dipping ones. One such low-angle fault, with a probably large down-to-the-east offset, is well-exposed at the entrance of Smith Creek canyon (Fig. 12a). The sharp fault plane separates a layer of brecciated limestones with steep, E-dipping cracks from a sheet of pulverized dolomite, 1–2 m thick, underneath (Figs. 11c and 12a). The most prominent examples of this geometry are found at the base of the upper plate where, as recognized by many authors (e.g. Wernicke 1981, Miller *et al.* 1983), most of the normal faults do not cut into the lower plate. The extensional faults which slice the Paleozoic carbonates generally sole into a layer of carbonate breccia located either at the

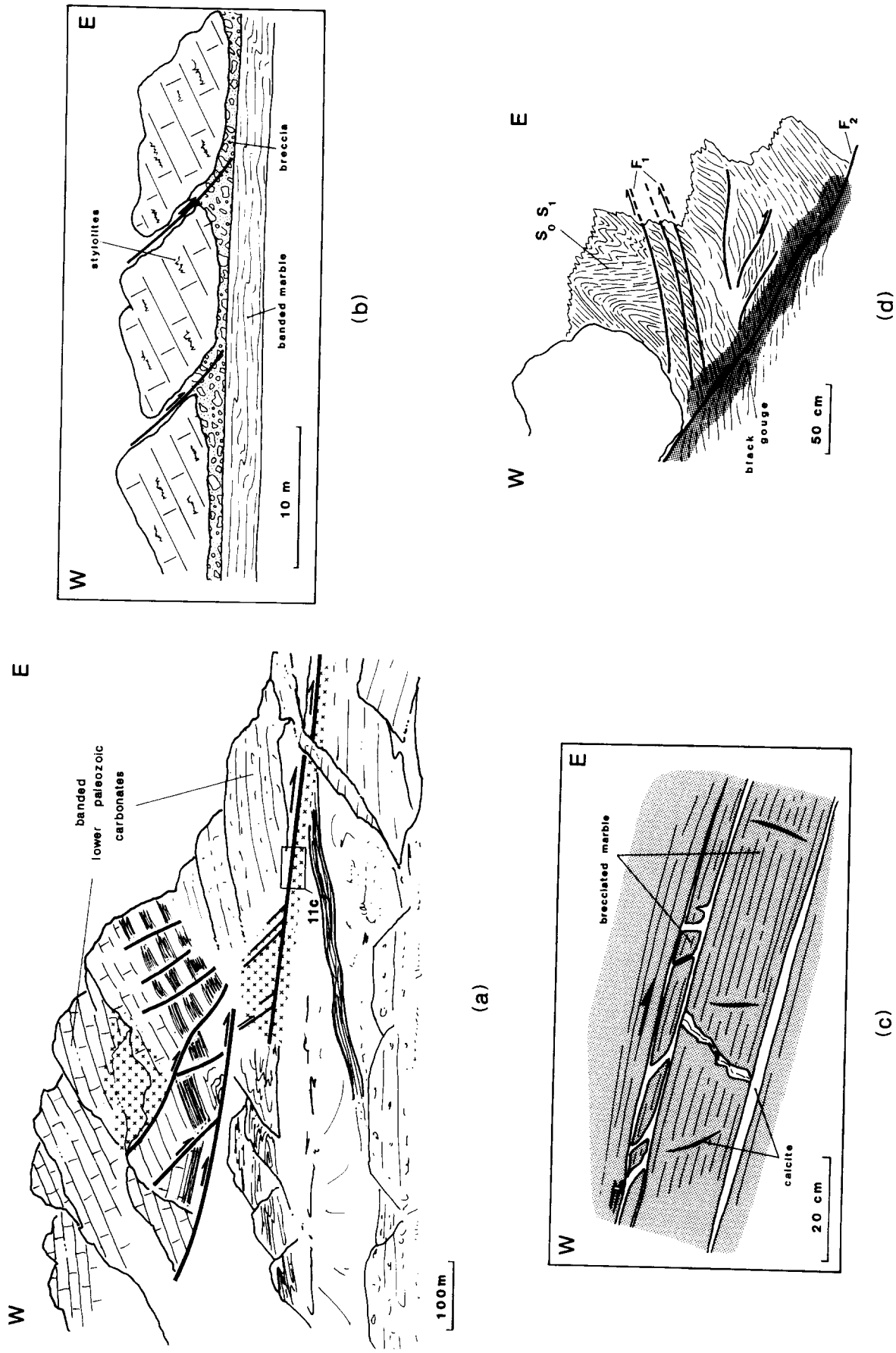

Fig. 12. (a) Large brittle normal faults in upper plate. Crosses indicate brecciated carbonates. Northward view near Smith Creek canyon outlet. (b) Schematic geometry of brittle fault junction with breccia layer on top of NSRD marble sheet. (c) Brittle deformation in brecciated marbles at base of NSRD marble sheet (Rock Canyon). (d) Relationships between folds and F_1, F_2 fault in Smith Creek (Fig. 11d). E-dipping faults (F_2) marked by black, cataclastic gouge, clearly postdate faults presently in reverse position (F_1).

very top of the NSRD marble sheet in the eastern part of the range (Fig. 12b), or on top of the quartzites in the southwest, where the marble tectonite is absent. This breccia, of variable thickness, contains angular, cm scale clasts of unmetamorphosed limestones and dolomites (Misch & Hazzard 1962, Nelson 1969, Miller *et al.* 1983). It resembles not only that found along large normal fault planes in the upper plate (Fig. 12a), but also that found in the olistolites embedded in the lacustrine limestones of the Sacramento Pass basin (Fig. 10). The contact between the breccia and the foliated marbles is usually quite sharp. Nevertheless, within the marbles, ductile shear planes parallel to the foliation appear to have been reactivated in a brittle way in places. Near the base of the marble sheet above Rock Canyon for instance, such planes are outlined by brown gouge and calcite, and the marble between them is brecciated and cut by calcite-filled gashes whose generally steeper eastward dip indicates small, down-to-the-east movements (Fig. 12c).

The typical way in which brittle faults in the upper plate merge with the breccia layer on top of the marble sheet is shown in Fig. 12(b), which is a sketch of particularly clear outcrops, west of Rock Canyon and in Smith Creek (Fig. 1). The faults, which separate blocks with comparable westward tilts, commonly meet the top surface of the marble at angles of 20 to 50°. The wedge-shaped footwall toes thus isolated usually appear to have suffered intense brittle deformation. They often correspond to gouge- and breccia-filled or even hollowed out triangular zones (Fig. 12b) as expected from compatibility requirements in 'domino-style' or 'deck of cards' models of extensional tectonics (e.g. Morton & Black 1975, Wernicke & Burchfiel 1982, Miller *et al.* 1983).

Probably not all the normal faults which disrupt the upper plate sole on top of the lower plate however. In addition to the faults which limit the northern Snake Range basement high to the east, west and south, large normal faults within the range may offset the décollement and descend into the lower plate. One such fault, outlined by steeply dipping upper plate strata, is clear just west of Mt Moriah on NHAP photos (Fig. 1). It appears to displace down-to-the-west lower plate quartzites in the upper reaches of Smith Creek, and to mark the western limit of the Silver Creek gneiss body and the Miller Basin Wash pelites (Fig. 1) (Stewart & Carlson 1978, Miller *et al.* 1983). Normal movement on this fault may account for the 600 m, down-to-the-west offset of the base of the upper plate between Hendrys and Negro Creeks (Miller *et al.* 1983, fig. 2) (Figs. 1 and 2a), as well as perhaps for the absence of the NSRD marble sheet in the latter.

DEFORMATION OF INTERMEDIATE STYLE

Near the intersection of Smith Creek and NSRD (Fig. 1), the brittlely faulted Paleozoic carbonates of the upper plate are separated from the NSRD marble sheet by a layer of recrystallized limestones, a few tens of metres thick. While not foliated as the marbles underneath, these limestones are strongly deformed and exhibit a dense stylolitic cleavage S_1 which strikes N20–30°E and dips 30–50°W on average (Fig. 11d). The cleavage is affected by tight folds with axial planes dipping steeply to the W and striking roughly N20°E. The fold, as well as S_1, are sliced by shallow W-dipping faults, whose presently reverse attitude is compatible with the geometry of the folds and the dip of the cleavage (Figs. 11d and 12d, F_1). Finally, both S_1 and the 'reverse' faults are cut by normal faults striking N–S to NE–SW and dipping 30–40°E (Fig. 12d, F_2). Drag along these faults appears to have bent the cleavage back into a nearly horizontal or even E-dipping attitude. The latter faults are also outlined by zones of brecciated limestone and black gouge which merge with a more prominent zone of cataclasis on top of the NSRD marble sheet, as in Fig. 12(b).

Except for the folds and stylolitic cleavage, the two-phase faulting sequence observed here resembles, on a small scale, that described by Miller *et al.* (1983, figs. 2 and 4), as typical of upper plate faulting. The second set of E-dipping, clearly brittle faults (F_2) which merge with the gouge layer on top of the marbles would correspond to second generation normal faults in Gans & Miller (1983) and Miller *et al.* (1983). The origin of the first generation, more ductile faults (F_1), and of the probably only slightly older schistosity and folds, is less clear. The fact, however, that beds in Paleozoic carbonates of the upper plate, above the layer of schistose limestones, are not strongly tilted and nearly parallel to the NSRD marble sheet suggests that strain-induced rotations, if any, have been restricted to that layer. Hence, depending on the amount of such rotations, there appear to be two extreme possibilities.

(i) If the stylolitic cleavage in the limestones initially formed roughly parallel to the bedding and to the NSRD marble sheet, local anticlockwise rotations linked with down-to-the-east normal movement on the E-dipping faults (F_2) could have reached 30–40°. The now W-dipping reverse faults (F_1) could thus have formed as shallow E-dipping shear zones analogous to those in Fig. 9(a). The stylolitic cleavage and the folds affecting it would then be less ductile analogs of, respectively, the foliation and the E-vergent folds observed in the NSRD marble sheet underneath (e.g. Figs. 5d–f, 6, 7 and 8c), and the two sets of faults would result from two successive phases of rotational boudinage, in keeping with the mechanism of Fig. 9(a). The main difference between such a deformation sequence and that discussed in Miller *et al.* (1983, fig. 4) would thus be its confinement to a rather thin layer of rocks, indicating localized E-vergent shear at the base of the upper plate.

(ii) On the other hand, in more brittle (transitional), less intensely deformed horizons above the NSRD shear zone, the original attitude of the stylolitic cleavage could have departed from that of the foliation in this zone, much as in C-S mylonites. In this event, the present westward dips of the cleavage could (within 10–20°) reflect that initial attitude, and the first generation faults

(F_1) could correspond to small shears parallel to the décollement or splaying upwards from it. The stylolites, the older set of faults and the folds would then all indicate a component of localized, partly ductile ≃E–W shortening not far above the NSRD shear zone. Whichever of the above hypotheses is correct, however, both imply eastward transport of the upper plate.

DISCUSSION

The original incentive for the present study was that low-angle discontinuities in the metamorphic core complexes of the Basin and Range might typify deformation processes representative of the late tectonics of high continental plateaus like Tibet. Hence, a better knowledge of the nature and variation with depth of mid-crustal strains in those core complexes might provide constraints on physical models of the thermomechanical evolution of high plateaus. In such plateaus, important crustal thickening over a wide area appears to be followed, some tens of million years later, by distributed normal faulting and crustal thinning over the same area (e.g. Molnar & Tapponnier 1978). The thinning, apparently driven by the excessive thickness of the crust, may follow the increased ductility of the warmed lower crust and/or a change in boundary conditions along one edge of the plateau (e.g. Molnar & Tapponnier 1978, 1981, Dalmayrac & Molnar 1981, Sbar 1982, Glazner & Bartley 1985). Although there is no direct evidence that Nevada was once as high as present day Tibet, several similarities between the two areas suggest that the Basin and Range might have been a high plateau in the Eocene, its presently well-developed extensional tectonics thus perhaps corresponding to some advanced stage of those now incipient in Tibet (e.g. Molnar & Chen 1983, Coney & Harms 1984). The crust of the Great Basin is warm and, despite considerable thinning (e.g. Coney & Harms 1984), still at least 25 km thick. Its average elevation is still high (about 1600 m) and its even higher rims (Wasatch Range, northern Rocky Mountains, and Sierra Nevada) limit, as in Tibet (Armijo *et al.* 1986), a vast area of essentially internal drainage, where widespread normal faulting has been more prominent than in adjacent regions.

The main goal of our work was thus, by documenting strains in rocks above, within, and below the NSRD, to obtain direct information on the nature, sense and compatibility of movements on and near this décollement. The characters and distribution of strain(s) near the NSRD are indeed, along with their age(s), the central issue in the current controversy surrounding the main extant models (low-angle normal fault, brittle–ductile transition, reactivated thrust) (Wernicke 1981, Allmendinger & Jordan 1981, Allmendinger *et al.* 1983, Miller *et al.* 1983, Bartley & Wernicke 1984, Gans *et al.* 1985). While our microstructural investigation is far from exhaustive, by supplementing the substantial field data gathered so far (Miller *et al.* 1983), it helps clarify several aspects of the tectonics of the northern Snake Range.

A major, ubiquitous feature of the *ductile deformation* in the lower plate is its homovergent rotational component at all scales. This deformation is thus clearly not coaxial: it is compatible with E-vergent shear and implies a large amount of transport of the upper plate in the direction of the stretching lineation (N115°E ± 10°). The NSRD itself is an outstanding shear zone: most of the plastic shear strain induced by the displacement between the upper and lower plates appears to have been localized in the layers of mylonites which outline the décollement at the top of the lower plate and display all the characteristic attributes of intense shear zones (foliation and stretching lineation with uniform attitudes, sheath folds, S and C′ planes, asymmetric boudinage at different scales, etc.). Large scale, asymmetric boudinage is the most prominent result of intense, progressive E-vergent shear in the NSRD tectonites. This boudinage appears to be well-developed not only in Marble Canyon, but also throughout the northeastern Snake Range, the surface of which roughly follows the marble sheet capping the lower plate (Fig. 1). Although recognized by early workers (e.g. Nelson 1969) and noted in more recent studies (e.g. Coney 1974), it has apparently not been the object of detailed structural observations, even by Miller, Gans and co-workers (1983, 1985). As is often the case in large shear zones, the magnitude of transport is difficult to assess from strain observations alone.

The existence of sheets of ultramylonites and the fact that probably only the effects of the latest stages of ductile deformation are visible in most of the marble horizons aggravates the difficulties inherent to the nature of the NSRD, a mostly bedding-parallel shear zone. The late boudinage in Marble Canyon alone would imply at least 2 km of transport if the shear strain necessary to dissociate the boudins ($\gamma \simeq 20$) were considered a minimum strain across the ≃100 m thick marble sheet. Thus, a lower bound for ductile displacement on the NSRD shear zone is probably on the order of several km. An amount of ductile eastward transport 10 times larger, as inferred from palinspastic reconstructions (Bartley & Wernicke 1984), seems unlikely, however.

Although E-vergent shear is clear throughout the lower plate, the amount of finite ductile strain decreases markedly with depth under the décollement (Miller *et al.* 1983), that is, predictably, away from the shear zone. Ductile strain also appears to have been much smaller in the quartzites of Negro Creek (Miller *et al.* 1983). Besides, the deformation there loses much of its non-coaxial character, and the marble sheet outlining the NSRD shear zone in most of the northern Snake Range is absent. This suggests that the Prospect Mountain quartzites just west of Mt Moriah were never in the vicinity of that prominent shear zone. In this region, the décollement must therefore either have ramped up or downsection and/or splayed into several smaller shear or fault zones, each absorbing only fractions of the total eastward transport and thus inducing less strain in adjacent rocks. Clearly, such fault zones could be normal

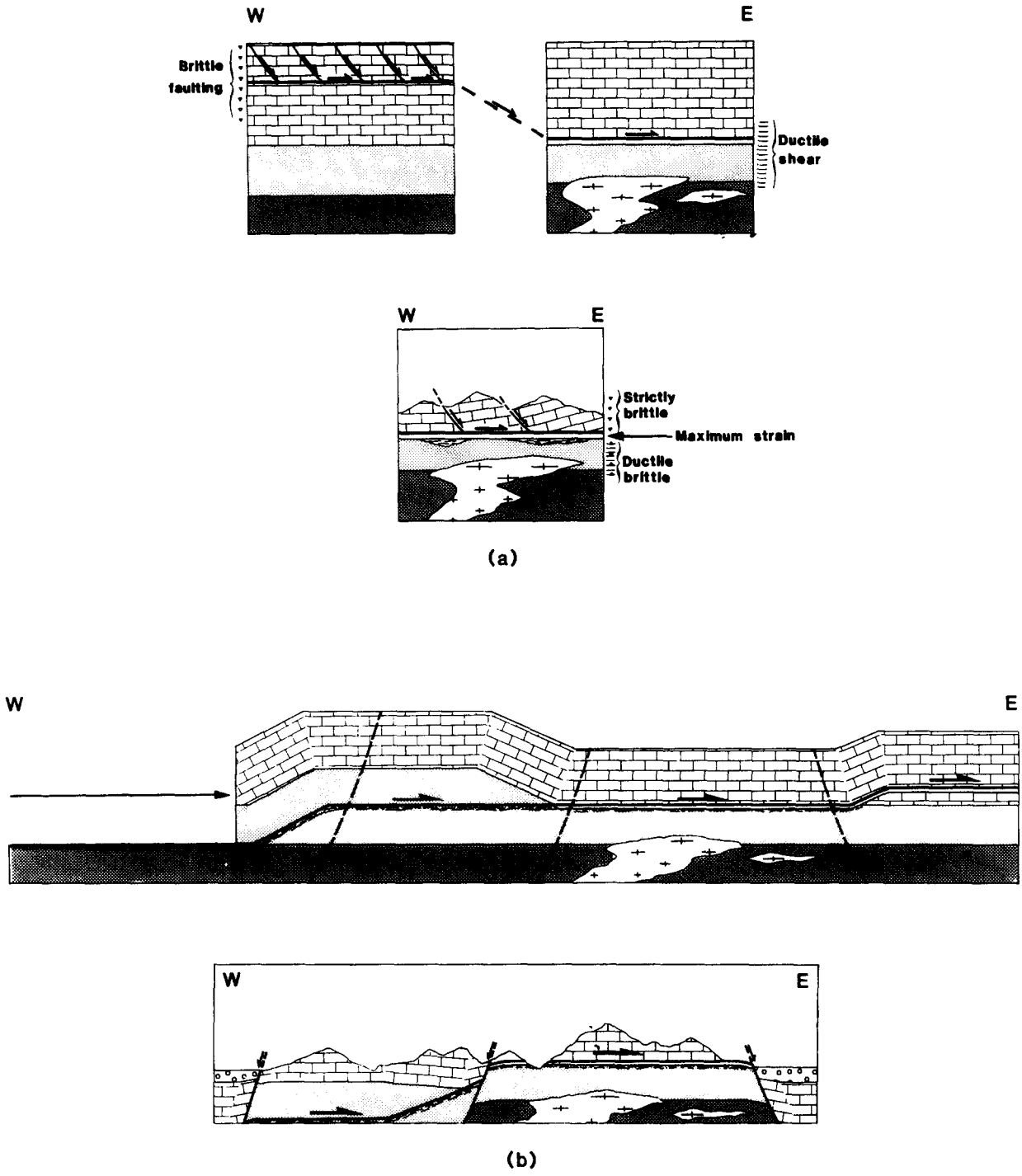

Fig. 13. Possible schemes for the tectonic evolution of the northern Snake Range Décollement (same lithologies as in Fig. 2): (a) As a low-angle normal fault cutting down-section towards the east (Wernicke 1981). Brittle deformation is in part late-stage of the ductile, deeper deformation. (b) As a deep thrust décollement during ductile, older phase, subsequently offset and uplifted by high-angle extensional faulting. Final reactivation as a brittle low-angle, normal décollement, with upper plate normal faults soling into breccia layer on top of marble sheet (Figs. 2a, 10b & c and 12b) is not shown.

faults in the upper plate, as depicted on most schematic sections (Wernicke 1981, Miller *et al.* 1983, Bartley & Wernicke 1984, Gans *et al.* 1985) (Fig. 13a). While the decrease of ductile strain with depth in the lower plate is gradual, the top surface of the NSRD marble sheet appears to mark, in general quite sharply (Miller *et al.* 1983), the upper limit of such strains. Except in Smith Creek canyon where schistose, recrystallized limestones are found above the breccia layer on top of the marble sheet, there is usually little evidence for behavior other than brittle above the marble–breccia contact. This is all the more remarkable since the most intense ductile deformation seems to have taken place in the marbles just below the contact, and implies that much of the hangingwall of the ductile shear zone is now missing (Fig. 13a).

In terms of strain, the NSRD is thus both an outstanding, narrow, E-vergent shear zone and a surprisingly

sharp contact between brittlely and ductilely deformed rocks. Either aspect apparently favors the shallow, E-dipping normal fault (Wernicke 1981) over the regional brittle–ductile transition model (Miller *et al.* 1983). A regional brittle–ductile transition zone some tens of metres wide seems hardly compatible with the rheological properties of quartz and calcite, while the low-angle normal fault model accounts for the juxtaposition of upper crustal, brittlely deformed hangingwall rocks with mid-crustal, ductilely deformed footwall rocks (e.g. Fig. 13a), for the eastward thinning of the lower plate quartzites, and for the westward decrease of strain in them (e.g. Bartley & Wernicke 1984). Moreover, since boudinage will occur principally in layers dipping in a direction—with respect to the shear plane—opposite to that of transport (Figs. 6 and 9a) (e.g. Ramsay 1967), the outstanding boudinage in the marble sheet implies that the NSRD must have cut down-section in the sense of transport (east) if the boudinaged layers correspond to the original stratification.

In spite of this seemingly concurrent evidence however, the low-angle normal fault model is not uniquely constrained by available structural data. In principle, because of the initial bedding shear-plane relationship noted above, the predominance of large scale asymmetric boudinage over folding could be used in a systematic way to differentiate low-angle normal from low-angle thrust shear zones throughout the Basin and Range. Such a predominance is indeed the main peculiarity of the NSRD compared with large thrust décollements from which it is otherwise indistinguishable in terms of strain. Unfortunately, this simple connection only holds if the boudinaged layering corresponds to near horizontal bedding prior to faulting. Any horizontal E-vergent shear zone initially cutting beds dipping, even slightly, to the west, or more generally any W-dipping E-vergent shear zone cutting beds with initially steeper westward dips would produce the observed boudinage and would be geometrically identical to the NSRD. Such a shear zone would in particular cut 'down' section, and juxtapose younger over older rocks. Yet it would in all probability be a thrust. Moreover, generally W-dipping strata should be the rule in the E-vergent Mesozoic Sevier Orogen. The very sharp transition from marbles to breccia poses problems even in the low-angle normal fault model. It implies that purely brittle movement on the NSRD must have been large and slow enough for the lower plate to have had little heat left to transfer into the uppermost part of the hangingwall. The strain rate singled out by Bartley & Wernicke (1984) ($5 \times 10^{-13} s^{-1}$, for 1–2 My) may thus be too fast by one order of magnitude or more. The kinematic link between brittle faulting in the upper plate and ductile shear in the lower plate poses further problems. The prominent E-dipping normal faults of the Egan and Schell Creek Ranges, originally a palinspastic key to large, down-to-the-east movement on the NSRD (Wernicke 1981), are now believed to have soled into another décollement, inferred to lie deep under the Snake Range (Bartley & Wernicke 1984). Besides, in contrast to what is shown in the section in Bartley & Wernicke (1984, Fig. 2), the NSRD appears to be cut by several prominent high-angle normal faults, in or along the edges of the Snake Range. The fact, in particular, that the Silver Creek Fault Zone offsets the NSRD casts doubts on the contemporaneity of ductile transport on it and movements on the Oligo-Miocene normal faults of the Sacramento Pass area.

Hence, it remains possible to ascribe ductile strains in the lower plate and NSRD tectonites on the one hand, and brittle faulting in both the upper and lower plates on the other hand to two distinct tectonic phases, under very different pressure-temperature conditions, rather than to a Tertiary extensional continuum. A sizeable lapse between two such phases would alleviate problems arising from the extreme sharpness of the brittle-ductile contact and from the fact that large, high-angle normal faults cut the ductile shear zone. As in the scenario first proposed by Misch (1960) and Misch & Hazzard (1962), the NSRD might have been a Mesozoic ductile thrust, later cut and brittlely reactivated by Tertiary extensional faulting. Ductile strains in the shear zone tectonites and underneath could thus be linked to Mesozoic shortening at the depths (10–15 km) required by the pressure (≈4 kb) and temperature (≈500°C) conditions of lower plate metamorphism (amphibolite facies) (Rowles 1982). Both the sense of transport and the direction of stretching lineation (roughly perpendicular to the Sevier Thrust Front) would be consistent with this inference. In this event, the NSRD shear zone could have ramped down under the quartzites of Negro Creek (fig. 13b) joining perhaps the deep, W-dipping reflector (K, fig. 3c from Gans *et al.* 1985) apparent on the SOHIO seismic profile in Spring Valley, then farther down under the Precambrian strata of the Schell Creek Range to the west. As major thrusts migrated towards the east in the Sevier Orogen (e.g. Burchfiel & Davis 1975), uplift and doming of the Snake Range could have started within a ramp anticline (above a deeper thrust) similar to those which have probably arched, along strike to the north, large metamorphic core complexes such as the Shuswap in the Canadian Cordillera (e.g. Mattauer *et al.* 1983, see also fig. 3 in Allmendinger & Jordan 1981). A few tens of million years later, Tertiary extension could therefore have been accommodated mostly by brittle normal faulting in either the upper or lower plate, already located at a higher, cooler level in the crust. Large, high-angle normal faults would have cut both plates and the ductile shear zone between them, contributing to the final uplift, doming and individualization of the Snake Range basement high (Fig. 13b). Several such faults however could have soled on top of the strain-hardened lower plate, thus producing the breccia layer, large tilts, and complexly attenuated upper plate 'chaos'. In the uppermost few km, such structures could in fact have originated mostly as large gravity slides (Misch 1960, Brun & Choukroune 1983), guided by the décollement or other stratigraphic interfaces in the upper plate. The presence of many large olistolites of upper plate carbonates, including tectonic breccia, in the Oligo-Miocene basins adjacent to the Snake Range supports this inference.

Moreover, the existence of such olistolites may alleviate one important difficulty, mentioned by Wernicke (1981), of mega-landslide models: shortening in the slide toes need not take place coevally with sliding of upper plate rocks, since such sliding may not occur in huge coherent sheets (Wernicke 1981, Fig. 3a) but rather in many successive avalanches feeding large and small clasts to the deposits in the basins. Since this mechanism is mostly a sedimentation process, the amount of extension in the upper plate veneer remaining on top of the ranges can be quite large if the adjacent basins are wide and deep, as implied by the relief and size of high-angle faults necessary to trigger the slides.

The most important difference between this latter scenario and those of Wernicke (1981), Davis (1983) or Miller *et al.* (1983), regarding the imbricate extensional faulting and attenuation, is the truly thin-skinned nature of that attenuation. Since it is restricted to the upper few km in the ranges, it does not require comparably large amounts of extension in the middle and lower crust. We suspect the extreme stretching of the Snake Range upper plate (500% according to Miller *et al.* 1983) to be in favor of extremely superficial attenuation, mostly by landsliding, although it is possible to argue that it might result from brittle simple shear (Bartley & Wernicke 1984). The chief distinction between Wernicke's or Davis' crustal thinning models, Miller's scenario for the attenuation of the Snake Range upper plate and asymmetric boudinage in the NSRD marble sheet (Fig. 9a) is the thickness of the layer involved, and thus it is especially important to determine the characteristic scale (50–500 m, 5–50 km?) of the most intense asymmetric boudinage to decide which of the above models is correct.

In the River Mts, southeast of Las Vegas, Nevada, a two-phase interpretation analogous to that outlined here is corroborated by the difference in brittle stretching and ductile transport directions (Choukroune & Smith 1985). In the northern Snake Range, a kinematic separation of possibly distinct phases on the basis of structural data alone is unfortunately more difficult. The ultimate test between the different models may thus lie in radiometric dating. The ages obtained so far yield an ambiguous picture. Zircons in the gneissic granites have U-Pb ages of ≈160 My (Lee *et al.* 1987) and the emplacement of some granites seems to have been coeval with E-vergent ductile shear. Micas in metamorphic pelites and diorites, on the other hand, give $^{39}Ar/^{40}Ar$, possibly cooling, ages as young as ≈22 My (Maluski, personal communication, Lee *et al.* 1987). If some of the gneissic granites were intruded in the Tertiary, high thermal gradients around them could have favoured local, albeit intense ductility, thus producing a contact-related, not regional, brittle–ductile transition and rehabilitating to some extent the hypothesis of Miller and co-workers (1983, 1985). In any event, the wide spectrum of ages implies a warm, slowly cooling crust between the Jurassic and the Miocene. Hence, whichever of Misch & Hazzard's or Wernicke & Miller's revisited models is more appropriate for the northern Snake Range, widespread low-angle normal faulting might characterize wide and high continental plateaux with a crust previously thickened—and consequently warmed—by low-angle thrusts.

Acknowledgements—Our fieldwork in the Snake Range was funded by grants from A.T.P. Géodynamique II of I.N.A.G., and A.S.P. Cordillères Américaines of C.N.R.S. This work benefitted from discussions with M. Mattauer, J. P. Brun, J. Malavieille, J. Van den Driessche. We also thank J. Aubouin, L. Montadert, and Ph. Gaudemer for additional support during the squeeze created by a soaring dollar. This is I.P.G.P. Contribution no. 819.

REFERENCES

Allmendinger, R. W. & Jordan, T. E. 1981. Mesozoic evolution, hinterland of the Sevier orogenic belt. *Geology* **9**, 308–313.

Allmendinger, R. W., Sharp, R. W., von Tish, D., Serpa, L., Kaufman, S., Oliver, J. & Smith, R. B. 1983. Cenozoic and Mesozoic structure of Basin and Range, Utah, from COCORP seismic reflection data. *Geology* **11**, 532–536.

Armijo, R., Tapponnier, P., Mercier, J. L. & Han Tong-Lin 1987. Quaternary extension in southern Tibet: field observations and tectonic implications. *J. geophys. Res.* In press.

Armstrong, R. L. 1972. Low-angle (denudation) faults, hinterland of the Sevier orogenic belt, eastern Nevada and western Utah. *Bull. geol. Soc. Am.* **83**, 1729–1754.

Bartley, J. M. & Wernicke, B. P. 1984. The Snake Range Décollement interpreted as a major extensional shear zone. *Tectonics* **3**, 647–657.

Berthé, D., Choukroune, P. & Gapais, D. 1979. Orientations préférentielles du quartz et orthogneissification progressive en régime cisaillant: l'exemple du cisaillement Sud-Armoricain. *Bull. Minéral.* **102**, 265–272.

Bouchez, J. L. 1977. Le quartz et la cinématique des zones ductiles. Thèse de Doctorat d'Etat, Université de Nantes, France.

Brun, J.-P. & Choukroune, P. 1983. Normal faulting, block tilting, and décollement in a stretched crust. *Tectonics* **2**, 345–356.

Burchfiel, B. C. & Davis, G. A. 1975. Nature and controls of Cordilleran orogenesis, western United States: extension of an earlier synthesis. *Am. J. Sci.* **275-A**, 363–396.

Choukroune, P. & Smith, E. I. 1985. Detachment faulting and its relationship to older structural events on Saddle Island, River Mountains, Clark County, Nevada. *Geology* **13**, 421–424.

Cobbold, P. R. & Quinquis, H. 1980. Development of sheath folds in shear regimes. *J. Struct. Geol.* **2**, 119–126.

Coney, P. J. 1974. Structural analysis of the Snake Range décollement, east-central Nevada. *Bull. geol. Soc. Am.* **85**, 973–978.

Coney, P. J. 1980. Cordilleran metamorphic core complexes: an overview. In: *Cordilleran Metamorphic Core Complexes* (edited by Crittenden, M. D. Jr, Coney, P. J. & Davis, G. H.). *Mem. geol. Soc. Am.* **153**, 7–31.

Coney, P. J. & Harms, T. A. 1984. Cordilleran metamorphic core complexes: Cenozoic extensional relics of Mesozoic compression. *Geology* **12**, 550–554.

Dalmayrac, B. & Molnar, P. 1981. Parallel thrust and normal faulting and constraints on the state of stress. *Earth Planet. Sci. Lett.* **55**, 473–481.

Davis, G. H. 1983. Shear zone model for the origin of metamorphic core complexes. *Geology* **11**, 342–347.

Gans, P. B. & Miller, E. L. 1983. Style of mid-Tertiary extension in east-central Nevada. *Utah Geol. Mineral Survey Spec. Studies* **59**, 107–160.

Gans, P. B., Miller, E. L., McCarthy, J. & Ouldcott, M. L. 1985. Tertiary extensional faulting and evolving ductile-brittle transition zones in the northern Snake Range and vicinity: new insights from seismic data. *Geology* **13**, 189–193.

Gapais, D. 1979. Orientations préférentielles de réseau et déformations naturelles, Thèse de 3° Cycle, Université de Rennes, France.

Glazner, A. F. & Bartley, J. M. 1985. Evolution of lithospheric strength after thrusting. *Geology* **13**, 42–45.

Grier, S. 1983. Tertiary stratigraphy and geologic history of the Sacramento Pass area, Nevada. *Utah Geol. Mineral Survey Spec. Studies* **59**, 139–144.

Hauser, E. C. 1985. The Schell Creek fault on the COCORP 40°N transect: a crustal scale normal fault. *Eos, Trans. Am. geophys. Un.* **66**, 979.

Hintze, L. H. 1980. Geologic map of Utah (1/500,000). *Utah Geol. Mineral Survey.*

Lacassin, R. & Mattauer, M. 1985. Kilometre-scale sheath folds at Mattmark, and implications for transport direction in the Alps. *Nature, Lond.* **315**, 739–742.

Laurent, Ph. & Etchécopar, A. 1976. Mise en évidence à l'aide de la fabrique du quartz d'un cisaillement simple à déversement ouest dans le massif de Dora Maira (Alpes occidentales). *Bull. Soc. géol. Fr. 7 Sér.* **18**, 1387–1393.

Lee, J., Miller, E. L., Marks, A. B. & Sutter, J. F., 1987. Ductile strain and metamorphism in an extensional tectonic setting: a case study from the northern Snake Range, Nevada, U.S.A. *J. geol. Soc. Lond.* In press.

Lister, G. S. & Snoke, A. W. 1984. S-C mylonites. *J. Struct. Geol.* **6**, 617–638.

Malavieille, J., Etchecopar, A. & Burg, J.-P. 1981. Analyse de la géométrie des zones abritées: simulation et application à des exemples naturels. *C. r. hebd. Séanc. Acad. Sci., Paris* **294**, 279.

Malavieille, J. 1982. Etude tectonique et microtectonique de la déformation ductile dans de grands chevauchements crustaux: exemples des Alpes franco-italiennes et de la Corse. Thèse de 3° Cycle, Université de Montpellier, France.

Mattauer, M., Collot, B. & Van den Driessche, J. 1983. Alpine model for the internal metamorphic zones of the North American Cordillera. *Geology* **11**, 11–15.

Miller, E. L., Gans, P. B. & Garing, J. 1983. The Snake Range Décollement: an exhumed mid-Tertiary ductile-brittle transition. *Tectonics* **2**, 239–263.

Misch, P. 1960. Regional structural reconnaissance in central-northeast Nevada and some adjacent areas—Observations and interpretations. In: *Geology of East-central Nevada, Intermountain Assoc. Petroleum Geologists*, 11th Ann. Field Conf. Guidebook, 17–42.

Misch, P. & Hazzard, J. C. 1962. Stratigraphy and metamorphism of late Precambrian rocks in central northeastern Nevada and adjacent Utah. *Bull. Am. Assoc. Petrol. geol.* **46**, 289–343.

Molnar, P. & Chen, W. P. 1983. Focal depths and fault plane solutions of earthquakes under the Tibetan Plateau. *J. geophys. Res.* **88**, 1180–1196.

Molnar, P. & Tapponnier, P. 1978. Active tectonics of Tibet. *J. geophys. Res.* **83**, 5361–5374.

Molnar, P. & Tapponnier, P. 1981. A possible dependence of tectonic strength on the age of the crust in Asia. *Earth Planet. Sci. Lett.* **52**, 107–114.

Morton, W. H. & Black, R. 1975. Crustal attenuation in Afar. In: *Afar Depression of Ethiopia, Inter-Union Commission on Geodynamics* (edited by Pilgar, A. & Rosler, A.). International Symposium on the Afar region and related problems, Proceedings, Scientific Report No. 14, 55–65.

Nelson, R. B. 1969. Relation and history of structure in sedimentary succession with deeper metamorphic structures, eastern Great Basin. *Bull. Am. Assoc. Petrol. geol.* **53**, 307–339.

Passchier, C. W. 1984. The generation of ductile and brittle shear bands in a low-angle mylonite. *J. Struct. Geol.* **6**, 273–281.

Platt, J. P. 1984. Secondary cleavages in ductile shear zones. *J. Struct. Geol.* **6**, 439–442.

Ramsay, J. 1967. *Folding and Fracturing of Rocks*. McGraw-Hill, New York.

Rowles, L. 1982. Deformational history of the Hampton Creek Canyon area, Northern Snake Range, Nevada. Unpublished M.S. Thesis, Stanford University, Stanford, California.

Sbar, M. L. 1982. Delineation and interpretation of seismotectonic domains in western North America. *J. geophys. Res.* **87**, 3919–3928.

Simpson, C. & Schmid, S. M. 1983. An evaluation of criteria to deduce the sense of movement in sheared rocks. *Bull. geol. Soc. Am.* **94**, 1281–1288.

Stewart, J. H. 1978. Basin-range structure in western North America: a review. In: *Cenozoic Tectonics and Regional Geophysics of the Western Cordillera* (edited by Smith, R. B. & Eaton, G. P.). *Mem. Geol. Soc. Am.* **152**, 1–32.

Stewart, J. H. & Carlson, J. E. 1978. Geologic map of Nevada (1/500,000). U.S. Geological Survey in cooperation with Nevada Bureau of Mines.

Wallace, R. E. 1978a. Patterns of faulting and seismic gaps in the Great Basin province. In: *Proc. Conf. VI, Methodology for Identifying Seismic Gaps and Soon-to-break Gaps*, May 25–27, 1978. *Open File Rep. U.S. geol. Surv.* **78–943**, 858–868.

Wallace, R. E. 1978b. Geometry and rates of changes of fault-generated range fronts, north-central Nevada. *J. Res. U.S. geol. Surv.* **6**, 637–649.

Wernicke, B. P. 1981. Low-angle normal faults in the Basin and Range Province: nappe tectonics in an extending orogen. *Nature, Lond.* **291**, 645–648.

Wernicke, B. P. & Burchfiel, B. C. 1982. Modes of extensional tectonics. *J. Struct. Geol.* **4**, 105–115.

Zoback, M. L., Anderson, R. E. & Thompson, G. A. 1981. Cainozoic evolution of the state of stress and style of tectonism of the Basin and Range province of the western United States. *Phil. Trans. R. Soc. Lond.* **A300**, 189–216.